

THE DIMER LOOP AND ELECTROSTATIC INTERACTIONS AT THE DIMER  
INTERFACE OF HUMAN GLUTATHIONE SYNTHETASE

A THESIS

SUBMITTED IN PARTIAL FULFILLMENT OF THE REQUIREMENTS  
FOR THE DEGREE OF MASTERS OF SCIENCE  
IN THE GRADUATE SCHOOL OF THE  
TEXAS WOMAN'S UNIVERSITY

DEPARTMENT OF CHEMISTRY AND BIOCHEMISTRY  
COLLEGE OF ARTS AND SCIENCES

BY

MARGARITA DE JESUS, B.S.

DENTON, TEXAS

DECEMBER 2012

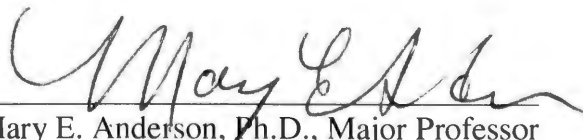
**TEXAS WOMAN'S UNIVERSITY LIBRARY**

TEXAS WOMAN'S UNIVERSITY  
DENTON, TEXAS

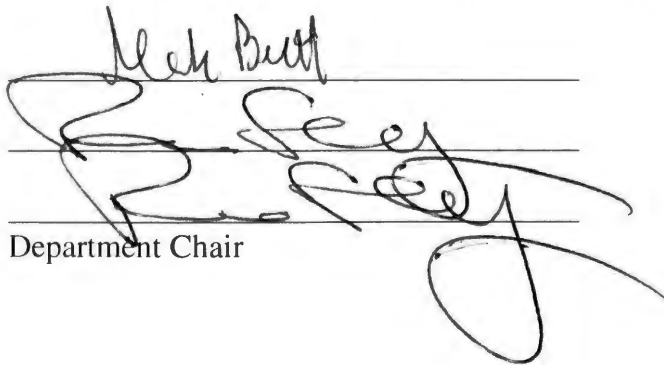
November 9, 2012

To the Dean of the Graduate School:

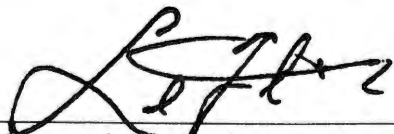
I am submitting herewith a thesis written by Margarita De Jesus entitled "The Dimer Loop and Electrostatic Interactions at the Dimer Interface of Human Glutathione Synthetase." I have examined this dissertation for form and content and recommend that it be accepted in partial fulfillment of the requirements for the degree of Master of Science with a major in Chemistry.

  
Mary E. Anderson, Ph.D., Major Professor

We have read this dissertation and recommend its acceptance:

  
Department Chair

Accepted:

  
Interim-Dean of the Graduate School

## DEDICATION

For Team GSH

## ACKNOWLEDGMENTS

Dr. Anderson, thank you for believing in me; thank you for seeing my potential and trying so very hard to make me the best scientist I can be. You will forever be my role model for a strong woman in science. You taught me to strive for the best, to probe every problem from all angles, and the importance of being meticulous. I believe I would be a very different person had you not asked me to be in your lab. Thank you for everything.

Dr. Cundari, your willingness to help me has never gone unappreciated. Thank you for your advice and words of encouragement. Of course, a big thanks for helping me with my research.

Teresa, you made me want to be a scientist. I will never forget how you inspired me to be what I am now and how you never let me give up, no matter how bad an experiment went. You taught me that if an experiment was salvageable it should be salvaged. You taught me the value of planning ahead and being prepared. Thank you.

Kerri, I do not know if you know this, but you are a great comfort to every person you interact with. You have never stopped supporting me. You knew when to put me in my place and knew when to build me up. Anytime I struggled with a research problem you were there to help, explain, or show me what I was doing wrong. Thank you for listening to me, whether it was research related or personal. Thank you for your help. Thank you for your friendship.

Bisesh, I would not have survived graduate school as well as I did without your help and support. Thank you for putting up with my craziness. I have never worked so well with someone as I have with you. Thank you for helping me when I needed it the most. You often knew I needed your help before I ever asked. Above anyone else in the lab, I could depend on you the most. You are as Dr. Anderson has said on many occasions my Bobbsey twin. Thank you.

Brandy, thank you for your help with my research; I would not be finishing now, if it were not for all your hard work. I have enjoyed the time we have worked together. Thanks for listening to me vent. Feel free to call and vent to me anytime.

Amy, I will never forget the times we spent troubleshooting our experiments together as Kerri looked on and giggled at us. You made lab fun and lighthearted for me. As we struggled through our experiments we would laugh and in the end we would inevitably accomplish what we set out to do. Thanks for your help and for your hard work.

I would also like to acknowledge the faculty and staff of the department of chemistry and biochemistry (you all have been so helpful and kind to me) as well as faculty members from the department of biology. I would like to especially thank, Dr. Sheardy, Dr. Britt, Dr. Webb, and Dr. Mills. Each of you have helped, provided suggestions, and encouraged me in my research during my undergraduate and graduate years here at Texas Woman's University. Thank you.

## ABSTRACT

MARGARITA DE JESUS

### THE DIMER LOOP AND ELECTROSTATIC INTERACTIONS AT THE DIMER INTERFACE OF HUMAN GLUTATHIONE SYNTHETASE

DECEMBER 2012

Human glutathione synthetase (hGS) is homodimeric and negatively cooperative toward its  $\gamma$ -glutamyl substrate making it a good model to study protein-protein interactions. The allosteric pathway between hGS active sites is hypothesized to travel through the dimer interface. To better understand the allostery of hGS and interactions at the dimer interface, two regions, the dimer loop [35-TSQEPTSSE-43] and key amino acid residues (Serine42, Arginine221 and Aspartate24) were studied using site-directed mutagenesis and analyzed for effects on cooperativity, activity and stability. Alanine mutant enzymes of dimer loop residues did not greatly affect activity or stability of hGS, nor change the cooperativity of hGS, but did affect  $\gamma$ -glutamyl substrate affinity, while alanine mutant enzymes of residues Ser42, Arg221 and Asp24 did not change cooperativity, but did decrease in activity and stability, and increase in  $\gamma$ -glutamyl affinity, with Asp24 having the greatest loss in activity and stability, followed by Arg221, and then Ser42.

## TABLE OF CONTENTS

	Page
DEDICATION .....	iii
ACKNOWLEDGMENTS .....	iv
ABSTRACT .....	vi
LIST OF SCHEMES .....	x
LIST OF TABLES .....	xi
LIST OF FIGURES .....	xii
 Chapter	
I. INTRODUCTION .....	1
Protein-protein Interactions .....	1
Cooperativity .....	1
Glutathione Synthetase .....	2
Human Glutathione Synthetase .....	3
Electrostatic Interactions and Dimer Loop of hGS .....	5
II. METHODOLOGY .....	7
Materials .....	7
Methods .....	7
Preparation of hGS Mutant Enzymes .....	7
Purification .....	8
Enzyme Assays and Kinetics Analysis .....	9
Differential Scanning Calorimetry .....	10
Circular Dichroism .....	10
Sequence Analysis .....	10
III. STRONG ELECTROSTATIC INTERACTIONS AT THE DIMER INTERFACE OF HUMAN GLUTATHIONE SYNTHETASE ARE ESSENTIAL FOR STABILITY BUT NOT ALLOSTERY .....	12
Summary .....	12

Introduction.....	13
Methods and Materials.....	17
Preparation of hGS Mutant Enzymes .....	17
Purification.....	17
Enzyme Assays and Kinetic Analysis.....	18
Differential Scanning Calorimetry (DSC) .....	18
Circular Dichroism.....	19
Computational Methods.....	19
Results.....	19
Analysis of Dimeric hGS Crystal Structure.....	19
Sequence Analysis .....	20
Ab Initio Calculation of Amino Acid Interactions .....	21
Experimental Activity and Kinetic Studies of hGS Mutant Enzymes.....	22
Temporal Analysis of Enzyme Activity .....	24
Experimental Measurement of Stability .....	25
Circular Dichroism, Secondary Structural Study.....	25
RMSD Analysis of Molecular Dynamics Geometries.....	26
Hydrogen Bond Analysis of Molecular Dynamics Geometries .....	26
Discussion .....	28
Acknowledgements.....	31
Footnotes.....	32
References.....	33
Supplemental Data .....	36
Computational Methods.....	36
Structural Analysis of hGS .....	36
Sequence Analysis .....	36
Ab Initio of Amino Acid Interactions.....	37
Molecular Dynamics Simulations.....	37
RMSD Calculations .....	38
Hydrogen Bond Analysis of Molecular Dynamics Structures...	38

IV.    PROPERTIES OF THE DIMER LOOP OF HUMAN GLUTATHIONE SYNTHETASE .....	47
Introduction.....	47
Methods.....	48
Results.....	48
Sequence Conservation .....	48
Activity and Kinetic Studies of hGS Mutant Enzymes .....	50
Experimental Measurement of Stability .....	52
Discussion .....	52



V. FUTURE DIRECTION .....	55
REFERENCES .....	56

## LIST OF SCHEMES

Scheme	Page
1.1 Biosynthesis of glutathione .....	3

## LIST OF TABLES

Table	Page
3.1. Comparison of the conservation of hGS residues near the dimer interface between higher eukaryotes and mammals .....	21
3.2. Activity, kinetic properties and thermal stability of hGS .....	24
S1. Primers for site directed mutagenesis of S42, R221 and D24 of glutathione synthetase.....	40
S2. RMSD of hGS mutants relative to wild-type hGS in Å .....	40
S3. Hydrogen bond analysis of wild-type and mutants hGS .....	41
4.1. Comparison of the conservation of hGS dimer loop residues between higher eukaryotes and mammals .....	50
4.2. Activity, kinetic properties and thermal stability of hGS enzymes .....	52

## LIST OF FIGURES

Figure	Page
1.1 Homodimeric human glutathione synthetase.....	4
1.2 Interactions across the dimer interface from chain A to chain B < 3 Å .....	6
3.1. Interaction energies across the dimer interface of hGS.....	22
3.2. Activity of wild-type and hGS mutant enzymes R221A and D24A over time.....	25
3.3. Hydrogen bonding in (a) wild-type hGS and (b) D24A hGS.....	27
S1. Homodimeric human glutathione synthetase.....	43
S2. Circular dichroism spectra of wild-type hGS and dimer interface hGS mutant enzymes (S42A, R221A and D24A) .....	44
S3. Hydrogen bonding in S42A mutant hGS.....	45
S4. Hydrogen bonding in R221A mutant hGS .....	46
4.1. The dimer loop (red) of hGS.....	47
4.2. Close-up view of the dimer loop (red) of hGS .....	48

## CHAPTER I

### INTRODUCTION

#### **PROTEIN-PROTEIN INTERACTIONS**

Protein-protein interactions are fundamental to the function of multimeric proteins, facilitating numerous cellular processes *e.g.*, cell communication through G protein coupled receptors, carbohydrate metabolism regulation by insulin, and chaperones assistance in the folding/unfolding of other macromolecules to name a few. Regulation of biological pathways is often carried out through protein-protein interactions that mediate ligand binding of a protein or enzyme (Haber & Koshland, 1967; Kirtley & Koshland, 1967). The protein-protein interactions that govern the function for many proteins are not well understood, such as the role these interactions have in allosteric regulation of an enzyme.

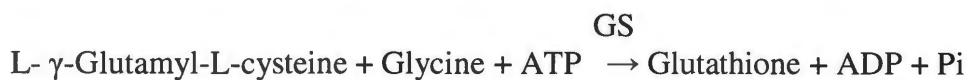
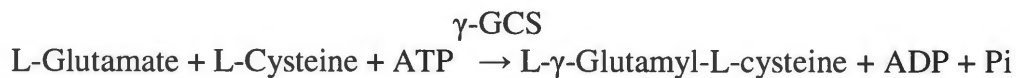
#### **COOPERATIVITY**

Allosteric regulation, *i.e.* cooperativity, is seen in enzymes or receptors that have multiple binding sites (*i.e.* multimeric) (Koshland & Hamadani, 2002). When a ligand binds to one of the binding sites of the enzyme or receptor, the affinity for another ligand to bind to the other binding site(s) is affected, either increasing (positive cooperativity) or decreasing (negative cooperativity) (Koshland & Hamadani, 2002). When cooperative binding occurs, proteins often display positive cooperativity. The most widely known and referenced display of positive cooperativity is that of oxygen binding to the tetrameric

protein hemoglobin. Studies of hemoglobin show that the binding of one oxygen significantly increases the affinity for additional oxygens to bind (Adair, 1925). The other form of cooperativity, negative cooperativity, is less common but becoming more recognized. Negative cooperativity is seen in receptors such as the insulin receptor (Winkle & Krugh, 1981) and aspartate receptor (Newton & Koshland, 1989), as well as in enzymes like malate dehydrogenase (Henis & Levitzki, 1980) and fumarase (Hasinoff & Davey, 1986). Cooperativity, especially negative cooperativity is not fully understood and further research into the process and the interactions that mediate this process is needed.

## **GLUTATHIONE SYNTHETASE**

Mammalian glutathione synthetase (GS), both human and rat are also examples of negatively cooperative enzymes. Glutathione synthetase catalyzes the second step in the biosynthesis of the essential antioxidant glutathione, by using ATP to ligate L- $\gamma$ -glutamyl-L-cysteine ( $\gamma$ -GC) and glycine (Huang, Meister, & Anderson, 1995) (Scheme 1). The rat and human species of GS are both homodimers and are negatively cooperative toward their  $\gamma$ -glutamyl substrate, so that the binding of one L- $\gamma$ -glutamyl-L-cysteine substrate reduces the affinity for a second to bind.



### SCHEME 1.1 Biosynthesis of glutathione.

Based on crystal structures, species of GS (*Escherichia coli* (Yamaguchi et al., 1993), *Saccharomyces cerevisiae* (Meister, 1974), *Arabidopsis thaliana* (Jez & Cahoon, 2004) and *Homo sapiens* (Polekhina, Board, Gali, Rossjohn, & Parker, 1999)) are members of the ATP-grasp superfamily of enzymes, that use ATP to form a bond between a carboxyl and an amino (or imino nitrogen for some other ATP-grasp proteins) (Galperin & Koonin, 1997; Meister, 1974; Jez & Cahoon, 2004; Galperin & Koonin, 2012). Other members of this family include enzymes involved in bacterial cell wall and nucleotide biosynthesis, popular targets for antibiotics (Fawaz, Topper, & Firestone, 2011). Human GS was the first and still is one of few known mammalian ATP-grasp enzymes (Galperin & Koonin, 1997; & Koonin, 2012). Thus, the allostery of GS as well as its place in the ATP-grasp superfamily makes the enzyme a promising candidate to study negative cooperativity and how GS compares structurally and functionally to other ATP-grasp enzymes.

### HUMAN GLUTATHIONE SYNTHETASE

As a homodimeric enzyme, human glutathione synthetase (hGS) is composed of two identical subunits (Polekhina et al., 1999) with active sites on each subunit (Fig 1.1). Each subunit is 474 amino acids long and has three catalytic loops, the G-loop (residues

366-375), the S-loop (residues 266-276) and the A-loop (residues 454-466) (Dinescu, Anderson, & Cundari, 2007). The distance from one active site to the other active site is  $\sim 40$  Å (Polekhina et al., 1999). Since hGS is negatively cooperative toward its  $\gamma$ -GC substrate, the active sites on each subunit must communicate to each other in a definite pathway (allosteric pathway). The allosteric pathway of hGS from one active site to the other therefore must cross through the dimer interface (residues 3-48). The focus of this study is on dimer interface of glutathione synthetase, an ideal area to study negative cooperativity and protein-protein interactions.

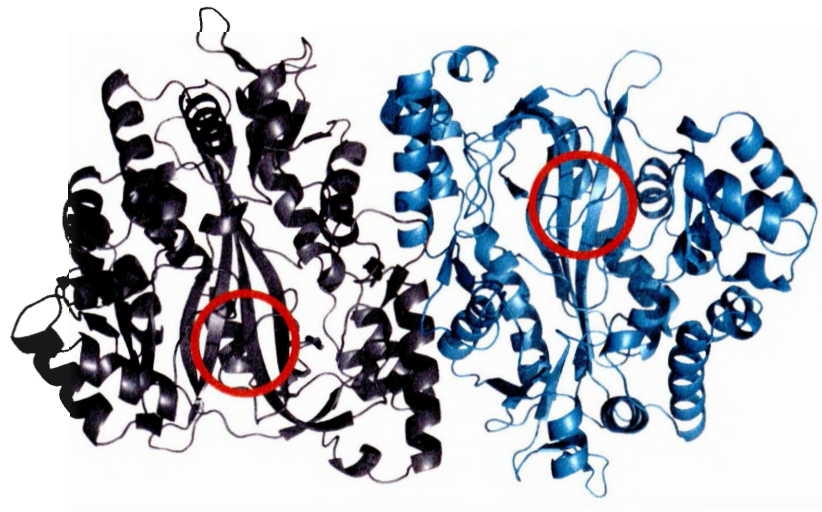


**FIGURE 1.1 Homodimeric human glutathione synthetase.** Chain A (gray ribbon) and chain B (cyan ribbon); active sites circled in red.



## **ELECTROSTATIC INTERACTIONS AND DIMER LOOP OF hGS**

Computational analysis of the hGS (by collaborators from CASCaM, University of North Texas) dimer interface shows key residues (S42, R221, and D24) that interact in electrostatic interactions (hydrogen bonds and a hydrogen-ionic interactions/salt bridges) across the interface from chain A to chain B  $< 3 \text{ \AA}$  apart (Fig 1.2) as well as the dimer loop [35-TSQEPTSSE-43] which is located at the interface. Both the key residues as well as the dimer loop may serve a role in hGS allostery and stability. Previous studies from our lab on the dimer interface of hGS (residues V44 and V45) suggest that the dimer interface is closely linked to the stability of the enzyme, and that the strength of interactions for residues at the interface is correlated with their impact on enzyme activity and stability (Slavens, Brown, Barakat, Cundari, & Anderson, 2011). The location of the dimer loop makes it ideal to study the effects of hGS cooperativity, and since the interactions of S42, R221, and D24 are shorter than the previously studied hydrophobic interactions at the interface of hGS. Thus it is reasonable to suggest that the interactions of S42, R221, and D24 may affect the stability and cooperativity of hGS more than the V44 and V45 interactions. Since D24 participates in two separate interactions across the interface, a salt bridge with R221 and an ionic hydrogen bond with S24, it is reasonable to hypothesize that D24 is the most important of these three dimer interface amino acid residues.

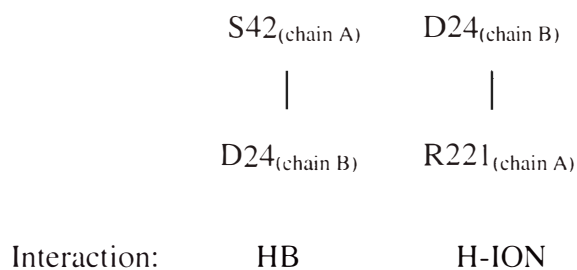


**FIGURE 1.2. Interactions across the dimer interface from chain A to chain B < 3 Å.**  
HB: hydrogen bond; H-ION: hydrogen-ionic interaction

The work presented in this thesis addresses the question: what role do the protein-protein interactions at the dimer interface of hGS serve? Do these interactions and the dimer loop directly participate in hGS cooperativity? The results of this study will give further insight into the allostery of hGS and the roles interface interactions have in hGS and possibly other multimeric enzymes.

## CHAPTER II

### METHODOLOGY

#### MATERIALS

Expression vector pET-15b, Escherichia coli XL1 Blue competent cells, and Ni-NTA His-Bind® resin are from Novagen, Inc. The primers are synthesized by Integrated DNA Technologies, Inc. (IDT). The QuickChange™ Site-Directed Mutagenesis Kit is from Stratagene, Inc. The Wizard® Plus Midipreps DNA Purification System is from Promega. The ampicillin and bovine serum albumin are from Sigma-Aldrich. Isopropyl-1-thio-β-galactopyranoside (IPTG) is from American Bioanalytical. L-γ-glutamyl-L-α-aminobutyrate (γ-GluABA) was from Bachem, Inc. Concentrators, 20K MWCO/ 7 ml, are from Pierce®. All other reagents, unless noted, are of the highest purity and purchased from Sigma-Aldrich, US Biological, Fisher Scientific or Amresco.

#### METHODS

*Preparation of hGS Mutant Enzymes*-Wild-type hGS is subcloned into a pET-15b expression vector with an N-terminal 6x histidine tag to yield hGS pET-15b (Dinescu, Cundari, Bhansali, Luo, & Anderson, 2004; Dinescu, Brown, Barelier, Cundari, & Anderson, 2010). PCR/ Site-directed mutagenesis is carried out with internal primers, then the hGS pET-15b DNA is transformed into *E. coli* XL1 Blue, purified with the Wizard® Plus Midipreps System, and the hGS insert sequence is confirmed by sequencing (GENEWIZ, Inc.). The hGS pET-15b plasmid DNAs are expressed in *E. coli*

BL21(DE3) cells as previously described (Dinescu et al., 2004; Dinescu et al., 2010) and summarized below.

*Purification*-BL21(DE3) cells containing wild-type or mutant hGS pET-15b vectors are grown with shaking (1 L Luria Broth media, 100 µg/ml ampicillin, 37 °C, 275 RPM) to an OD<sub>600</sub> of 0.8 to 1.0 (~ 4 hours); chill at 4°C for 30 min, induce with IPTG (~0.80 mM) at 19 °C for 4 hrs with shaking (275 rpm).

All procedures are carried out at 4 °C. Following induction, the cells are centrifuged (10 min, 5,000 x g), washed with cold saline (0.85% NaCl, 15 mL), and centrifuged (10 min, 5,000 x g). The cell pellets (~ 9.0 gm) are lysed (Constant Cell Disruption System model: 01/40/BA) at 15,000 psi, in MCAC-0 buffer, pH 8.0 (20 mM Tris-Cl, 0.5 M NaCl, and 10% glycerol) followed by sonification (Branson D450 Sonifier; 2 min total: 0.5 s pulse, 0.5 s rest, 35% amplitude). After centrifugation (10,000 x g, 4 °C, 20 min), the supernatant is applied to a metal chelate affinity chromatography column (1.5 x 15 cm, Ni-NTA His-Bind® resin), and is washed (MCAC-0 buffer) until OD<sub>280</sub> returned to baseline; washed with MCAC 55 (MCAC-0 + 55 mM imidazole) buffer until baseline again. The hGS enzymes are eluted with MCAC-100 (MCAC-0 + 100 mM imidazole) collected in 2 to 4 mL fractions. The purified hGS enzymes are dialyzed (2 x 4 L) overnight in Tris buffer (20 mM Tris-Cl and 1 mM EDTA, pH 8.6). The hGS enzymes are pure by SDS-PAGE (Dinescu et al., 2004; Dinescu et al., 2010). Protein concentration is determined by the Lowry method, using bovine serum albumin as the standard (Lowry, Rosebrough, Farr, & Randall, 1951).

*Enzyme Assays and Kinetic Analysis*-Activity of purified hGS enzymes is measured using a pyruvate kinase (PK) / lactate dehydrogenase (LDH) coupled assay as previously described (Dinescu et al., 2004; Dinescu et al., 2010). To avoid complications of oxidation of the  $\gamma$ GC thiol, L- $\gamma$ -glutamyl-L- $\alpha$ -aminobutyrate ( $\gamma$ -GluABA), an analog of  $\gamma$ -glutamylcysteine ( $\gamma$ GC) with the same activity and kinetic properties as  $\gamma$ GC was used (Oppenheimer, Wellner, Griffith, & Meister, 1979). The reaction is initiated by the addition of the purified recombinant hGS to a pre-incubated (37 °C, 11 minutes) standard reaction mixture (0.2 mL final volume) containing 100 mM Tris-Cl pH 8.2 (25 °C), 50 mM KCl, 20 mM MgCl<sub>2</sub>, 5 mM PEP, 10 units/assay LDH type II from rabbit muscle, 10 units/assay PK type II from rabbit muscle, 0.2 mM NADH, 10 mM each of ATP, glycine, and  $\gamma$ -GluABA. The rate of the reaction is monitored continuously at 340 nm to determine the rate of NADH oxidation. A unit of activity is the amount that catalyzes 1  $\mu$ mole of product per minute at 37.0 °C.

Kinetic parameters are determined using the standard assay conditions as described above with varying the concentration of the substrate of interest. The  $K_m$  is determined by keeping two substrates at constant saturation and varying the third substrate to at least 10-fold above and below the approximate  $K_m$ . To ensure the activity is  $\gamma$ -GluABA dependent, control reactions are run in the absence of  $\gamma$ -GluABA. Sigma Plot 11.0 software is used to calculate and determine Hill coefficients,  $K_m$  and  $V_{max}$  (Dinescu et al., 2004; Dinescu et al., 2010).

*Differential Scanning Calorimetry*-Enzymes are dialyzed overnight (2 x 4 L, 4 °C) in Tris buffer, and then concentrated (~1.0 - 2.0 mg/mL). Differential scanning calorimetry scans are carried out (Calorimetry Sciences Nano Series III instrument, 1.0 atm, rate of 1.0 °C/min, 10 - 90 °C) and baseline corrected against dialysate after being degassed for 15 min.

*Circular Dichroism*-Enzymes were dialyzed overnight in sodium phosphate buffer (10 mM, pH 7.5, 2 X 1 L, 4 °C). Measurements were carried out on an OLIS RSM 1000 with DSM CD attachment from 260 to 190 nm (4 °C) with an integration time of 2 s (0.2 cm round quartz cuvette). The buffer spectrum was subtracted from the enzyme spectra. The Savitsky–Golay algorithm (19) was used to smooth data (RC filter – 13; digital filter –17) during acquisition and analysis with OLIS GlobalWorks software. Data was converted to molar ellipticity ( $\text{deg. cm}^2 \text{dmol}^{-1}$ ) and represent an average of at least 5 scans.

*Sequence Analysis*-Utilizing the NCBI database, the sequence of hGS (2HGS) was matched to known protein sequences using BLAST and a non-redundant database and aligned using the BLOSUM62 matrix (Altschul et al., 1997; Berman et al., 2000; Meng, Pettersen, Couch, Huang, & Ferrin, 2006). Hypothetical and theoretical sequences were eliminated from the alignment. Conservation was determined for all higher eukaryote and all mammalian sequences. Percent conservation of each residue was calculated relative to wild-type hGS. Percent charge conservation at each site was also calculated assuming biological pH of 7.6. Aspartic and glutamic acid side chains were

assumed to be negatively charged, while arginine and lysine were treated as positively charged. All other amino acids were considered neutral.

## CHAPTER III

# STRONG ELECTROSTATIC INTERACTIONS AT THE DIMER INTERFACE OF HUMAN GLUTATHIONE SYNTHETASE ARE ESSENTIAL FOR STABILITY BUT NOT ALLOSTERY

Margarita C. De Jesus, Brandall L. Ingle, Khaldoun A. Barakat, Bisesh Shrestha, Kerri D. Slavens, Thomas R. Cundari, Mary E. Anderson

A paper to be published in The Journal of Biological Chemistry (2012)

**Keywords:** Glutathione synthetase; protein-protein interactions; negative cooperativity; multimeric proteins; ATP-grasp enzymes; allosteric regulation; cooperativity; glutathione; metabolism

**Background:** Human glutathione synthetase (hGS) participates in the synthesis of the antioxidant glutathione.

**Results:** Point mutations at the dimer interface of hGS decreases enzyme activity and stability, without impacting allostery.

**Conclusion:** Electrostatic interactions across the hGS interface maintain enzyme.

**Significance:** Strong salt bridges and ionic hydrogen bonds are essential to multimeric enzyme stability, but likely do not participate in allosteric pathways.

## SUMMARY

Glutathione synthetase (GS) catalyzes the second step in the biosynthesis of glutathione, an important antioxidant. Wild-type human glutathione synthetase (hGS) is



homodimeric and negatively cooperative toward its  $\gamma$ -glutamyl substrate, making it an excellent model to study protein-protein interactions. The allosteric pathway between hGS active sites is posited to travel through the dimer interface. Integrated experimental and modeling studies show that charged/polar dimer interface amino acid residues S42, R221 and D24 play a significant role in monomer:monomer interactions in hGS. Using site-directed mutagenesis, these interface residues were changed to alanine and then analyzed to assess impact upon hGS activity, stability, and cooperativity. Mutant analysis shows that these amino acids at the dimer interface of hGS are necessary for its stability and their mutation alters  $\gamma$ -glutamyl substrate affinity, suggesting that both the local and global geometry of hGS are affected, but that these three polar dimer interface residues do not lie along the allosteric pathway of this negatively cooperative enzyme.

## **INTRODUCTION**

Numerous cellular processes are facilitated by protein-protein interactions, *e.g.*, cell communication through G protein coupled receptors, carbohydrate metabolism regulation by insulin, oxygen transportation by hemoglobin, and chaperones assistance in the folding/unfolding of other macromolecules to name a few. Regulated pathways are often modulated allosterically via ligand-protein interactions that are mediated by protein-protein interactions (1,2).

Two allosteric proteins, hemoglobin and aspartate transcarbamoylase (ATCase), are classic examples of positively and negatively cooperative proteins, respectively, and proteins that exhibit protein-protein interactions. Hemoglobin displays positive

cooperativity, increasing the affinity for subsequent oxygen binding once the initial oxygen binds to the heme (3). ATCase (*E. coli*) catalyzes the first step of pyrimidine biosynthesis, and is regulated by both positive (ATP) and negative (CTP) cooperativity as part of a feedback mechanism for maintaining a balance between cellular purine and pyrimidine pools (4,5). The function of allosteric proteins, like the aforementioned, is contingent on protein conformational changes caused by ligand binding of one subunit, which alters the ligand binding to other subunit/s, and is mediated by protein-protein interactions. Protein-protein interactions are involved in a variety of biological functions and increasingly are drug targets in the treatment of cancers, autoimmune diseases and bacterial infections (6,7). The precise relationship between protein-protein interactions and cooperativity remains a subject of great debate and study (8-10).

The homodimer human glutathione synthetase (hGS), a member of the ATP-grasp superfamily, catalyzes the second step in the biosynthesis of the essential antioxidant glutathione, by using ATP to ligate  $\gamma$ -glutamylcysteine and glycine; hGS is an allosteric enzyme (11). Human GS is negatively cooperative toward its  $\gamma$ -glutamyl substrate. When the first substrate binds, the affinity for substrate in the second subunit of hGS decreases, and down-regulates hGS activity and limits intracellular glutathione levels (12). Communication from one active site to the other must travel across the dimer interface, making this interface is an ideal area to study the negative cooperativity of hGS, its effect on regulation of cellular glutathione levels, and its relevance to the ATP-grasp superfamily.

Glutathione plays a key role in relieving oxidative stress within cells. Patients with genetic mutations leading to glutathione synthetase deficiencies suffer from a variety of symptoms, notably hemolytic anemia and neurological disorders (13). Neurons are especially sensitive to necrosis and apoptosis due to oxidative stress. It follows, therefore, that glutathione deficiencies have been associated in patients with Parkinson's disease, Alzheimer's disease and Lou Gehrig's disease (14). Glutathione deficiencies are associated with a variety of other diseases including diabetes, cystic fibrosis, HIV/AIDS and heart disease (15,16).

Human GS, like all members of the ATP-grasp family, uses ATP to form a bond between a carboxyl carbon and an amino (or imino nitrogen for some other ATP-grasp proteins) (17). As shown for yeast (18), and supported by a *arabidopsis thaliana* study (19), the hGS reaction is thought to proceed through an acyl phosphate intermediate. Structurally, hGS is similar to other members of the ATP-grasp superfamily of enzymes with a characteristic ATP-grasp fold (20). Members of this family include enzymes involved in bacterial cell wall and nucleotide biosynthesis, popular targets for antibiotics (21). Human GS was the first and still is one of few known mammalian ATP-grasp enzymes (17,20). Thus, structural and functional similarities as well as differences between hGS and other ATP-grasp enzymes make it an excellent model for study.

Our group's recent research on hydrophobic interactions at the dimer interface of hGS highlights the importance of interface interactions for this enzyme (22).

Hydrophobic residues V44 and V45 interact from chain A to chain B, and thus across the

dimer interface (V44<sub>A</sub>...V44<sub>B</sub> and V45<sub>A</sub>...V45<sub>B</sub>) with  $\alpha$ -carbon distances of 6.6 Å and 5.7 Å, respectively. All V44/45 mutations affected cooperativity, indicating that these residues are located along the allosteric pathway. V45 mutant hGS enzymes had lower activity and decreased stability compared to V44 mutants. The research indicated the dimer interface is closely linked to the stability of the enzyme, and that the strength of interactions for residues at the interface is correlated with their impact on enzyme activity and stability (22). Our recent findings thus suggest the dimer interface plays an important role in hGS activity and that further analysis of the dimer interface will yield better understanding of hGS, its properties, glutathione synthesis, regulation of, and information about allostery.

The computational analysis of hGS reported in this paper indicates that amino acid residues S42 and R221 interact strongly (separations < 3 Å) with D24 at the dimer interface. These interactions are shorter than the V44/45 hydrophobic interactions previously studied (22), suggesting that D24, S42 and R221 interactions may be crucial to the allostery and/or stability of hGS. Since D24 participates in two separate interactions (a salt bridge with R221 and an ionic hydrogen bond with S42) it is reasonable to hypothesize that it is the most important of these three dimer interface residues. The present research delineates the function of the interactions of dimer interface residues (S42, R221 and D24) and the important role that dimer interface interactions have in terms of activity, cooperativity, and stability of human glutathione synthetase.

## METHODS AND MATERIALS

Expression vector pET-15b, *E. coli* XL1 Blue competent cells, and Ni-NTA His-Bind® resin were from Novagen, Inc. The primers were synthesized by Integrated DNA Technologies, Inc. The QuickChange™ Site-Directed Mutagenesis Kit and Wizard® Plus Midipreps DNA Purification System were obtained from Stratagene, Inc. and Promega, respectively. American Bioanalytical supplied the Isopropyl-1-thio-β-galactopyranoside (IPTG). L-γ-glutamyl-L-α-aminobutyrate (γ-GluABA) was synthesized (12) or obtained from Bachem, Inc. Protein concentrators were from Pierce Inc. All other reagents, unless noted, were of the highest purity and obtained from Sigma-Aldrich, US Biological, Fisher Scientific or Amresco.

*Preparation of hGS Mutnat Enzymes*-Wild-type hGS in pET-15b expression vector has an N-terminal 6x histidine tag (hGS-pET-15b (23-25)). PCR/site-directed mutagenesis was carried out with internal primers (Table S1, Supplemental Material). The hGS wild-type and mutant cDNA sequences were confirmed by sequencing (GENEWIZ, Inc.). The hGS-pET-15b plasmid DNAs were expressed in *E. coli* BL21(DE3) cells (23,24).

*Purification*-Wild-type and mutant enzymes were purified as previously reported (22) and described here in brief. All procedures were at 4 °C. After induction, cells were washed with cold saline, and centrifuged. The cell pellets were lysed in MCAC-0 buffer (pH 8.0, 20 mM Tris-Cl, 0.5 M NaCl, containing 10% glycerol), sonicated (Branson D450 Sonifier), and centrifuged. The supernatant was applied to a His-tag affinity

chromatography column , and washed (MCAC-0 buffer), washed with MCAC-55 and hGS enzymes eluted with MCAC-100. The purified hGS enzymes were dialyzed overnight in Tris buffer (20 mM Tris-Cl and 1 mM EDTA, pH 8.6) and were pure by SDS-PAGE (22,23). Protein concentration was determined using Lowry method (26), with bovine serum albumin as standard.

*Enzyme Assays and Kinetic Analysis*-Activity of purified hGS enzymes was measured using a pyruvate kinase (PK)/lactate dehydrogenase (LDH) coupled assay as previously described (22-24). To avoid complications of oxidation of the  $\gamma$ GC thiol, L- $\gamma$ -glutamyl-L- $\alpha$ -aminobutyrate ( $\gamma$ -GluABA), an analog of  $\gamma$ -glutamylcysteine ( $\gamma$ GC) with the same activity and kinetic properties as  $\gamma$ GC was used (12). The reaction was initiated by addition of purified recombinant hGS to a pre-incubated standard reaction mixture. The reaction rate was monitored continuously at 340 nm. A unit of activity catalyzes 1  $\mu$ mol of product/min at 37.0 °C.

Kinetic parameters ( $K_m$ , Hill Coefficients) were determined using the standard assay above with varying concentrations of  $\gamma$ -GluABA to at least 10-fold above and below the approximate  $K_m$  while keeping the concentration of glycine and ATP constant. Control reactions were run in the absence of  $\gamma$ -GluABA. Sigma Plot 11.0 software was used to calculate and determine Hill coefficients,  $K_m$  and  $V_{max}$  (22-24).

*Differential Scanning Calorimetry (DSC)*-Enzymes were dialyzed overnight and concentrated (22). Scans were carried out (Calorimetry Sciences Nano Series III, 1.0 atm,

rate of 1.0 °C/min, 10 - 90 °C) and baseline corrected against dialysate after being degassed for 15 min.

*Circular Dichroism*-Enzymes were dialyzed overnight in sodium phosphate buffer (10 mM, pH 7.5, 2 X 1 L, 4 °C). Measurements were carried out on an OLIS RSM 1000 with DSM CD attachment (260 to 190 nm) as previously described using OLIS GlobalWorks software for analysis (25). Data was converted to molar ellipticity (deg. cm<sup>2</sup> dmol<sup>-1</sup>) and represent an average of at least 5 scans.

## COMPUTATIONAL METHODS

A combination of bioinformatics, *ab initio* calculations and molecular dynamics, was used to computationally probe the sequence and structure of hGS. A complete description of computational methods is found in the supplementary material. The techniques used were similar to previously published work by this group (22,23,27).

## RESULTS

*Analysis of Dimeric hGS Crystal Structure*-Analysis of dimeric hGS was initiated by looking for strong contacts between chain A and chain B amino acids across the dimer interface of 2HGS (28). Initial screens started with interactions of 4 Å or less) and the residue sets were then culled by reducing the threshold distance. Selected distances used are as follows (number of residues within specified distance is also denoted): (a)  $\leq 3.95$  Å, 28 residues per monomer, (b)  $\leq 3.50$  Å, 24 residues from each monomer, and (c)  $\leq 3.00$  Å, 5 residues from each monomer.

The above data show that the number of hGS residues that are close to the dimer interface falls off rapidly as the threshold distance is reduced. Moreover, the closest chain A:chain B interactions, and presumably the most chemically and biologically significant, are small in number. The five residues (D24, S42, E43, Y47 and R221 in both chains A and B of hGS) with the most significant bonding across the dimer interface were considered the initial target residues for study. Along with these five residues, V44 and V45 have the closest hydrophobic contacts across the dimer interface of 6.6 Å and 5.7 Å respectively (22). The importance of V44 and V45 for hGS activity and cooperativity was discussed in a recent paper (22). The seven residues participate in five significant dimer interface interactions (S42...D24, Y47...E43, R221...D24, V44<sub>A</sub>...V44<sub>B</sub> and V45<sub>A</sub>...V45<sub>B</sub>) (the subscript letters denoting the chain that residue belongs). Molecular dynamics analysis indicates that the Y47...E43 interaction is less important than the others. Hence, the remainder of the discussion focuses primarily on the S42...D24 and R221...D24 interactions at the dimer interface of hGS.

*Sequence Analysis*- Sequence analysis of hGS with glutathione synthetase of higher eukaryotes (prokaryotes display significantly greater sequence variability, data not shown) showed an average conservation of 43% and an average charge conservation of 60%. Among mammals, the average conservation of all amino acids in hGS is 71% (average charge conservation: 76%), Table 3.1. Polar residues S42, R221 and D24 show sequence conservation comparable to hydrophobic dimer interface V44 and V45, which were shown in previous research (22) to play important roles in maintaining



subunit:subunit interaction. The high conservation of S42 D24 and R221 suggests that there is a drive to conserve these residues across species. The overall and charge conservation of the latter two residues also leads to the hypothesis that the D24···R221 interchain salt bridge between plays an important role in hGS function and stability.

**TABLE 3.1**

**Comparison of the conservation of hGS residues near the dimer interface between higher eukaryotes and mammals.**

<b>Residue</b>	<b>Higher Eukaryotes*</b>		<b>Mammals</b>	
	<b>%C</b>	<b>%CC</b>	<b>%C</b>	<b>%CC</b>
<b>D24</b>	63.4	64.6	71.4	71.4
<b>S42</b>	24.4	59.8	61.9	66.7
<b>E43</b>	7.3	14.6	23.8	52.4
<b>V44</b>	39.0	51.2	66.7	76.2
<b>V45</b>	15.9	51.2	61.9	76.2
<b>Y47</b>	22.0	81.7	81.0	81.0
<b>R221</b>	40.2	40.2	71.4	71.4
<b>Ave</b>	42.6	60.3	70.5	76.0
<b>St Dev</b>	18.2	19.8	17.3	11.2

\*Higher eukaryotes include species from the Plantae and Animalia kingdoms; %C = conservation; %CC = charge conservation (positive, negative or neutral); Ave = average conservation for all amino acids relative to hGS. St Dev = sample standard deviation.

*Ab Initio Calculation of Amino Acid Interactions*-Several important points emerge from the *ab initio* residue:residue interaction energy data, Fig. 3.1. First, the effect of medium (*cf.* gas-phase and aqueous energies) is significant. Solvent shielding, particularly on the R221···D24 interchain salt bridge interaction, is substantial. Hence, solvent molecules (*in vivo* or *in vitro*) and solvent polarity will significantly attenuate

dimer interface interactions in hGS. Second, the calculated salt bridge (R221 $\cdots$ D24) interaction energy is double the binding energy of the S42 $\cdots$ D24 hydrogen bond in aqueous environment (-13.5 versus -6.1 Kcal/mol), suggesting that the salt bridge contact is the most substantial across the dimer interface of hGS. Third, D24 participates in both a strong salt bridge with R221, and a strong hydrogen bond with S42. Hence, D24 is the most interesting target for site directed mutagenesis experiments, and its mutation is expected to engender more substantial changes to hGS than mutation of the other dimer interface residues.

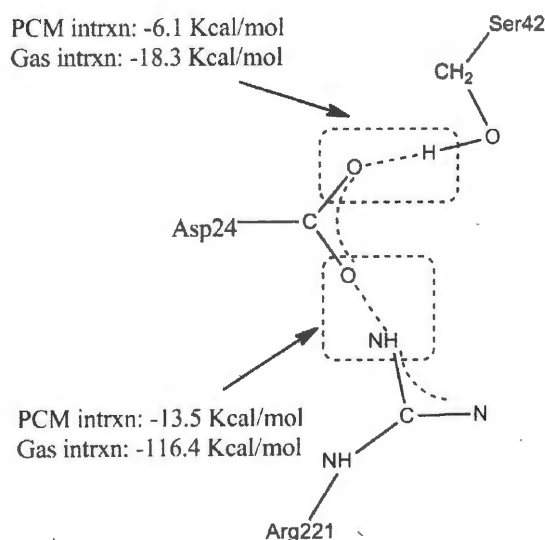


**FIGURE 3.1. Interaction energies across the dimer interface of hGS.** Calculated with B3LYP/6-31+G(d) for amino acids S42, R221 and D24 across the dimer interface of hGS in the gas and PCM (aqueous) phase

*Experimental Activity and Kinetic Studies of hGS Mutant Enzymes*-The functional effects of these dimer interface mutations (S42A, R221A and D24A) relative to wild-type

were assessed by activity:  $k_{\text{cat}}$  ( $\text{s}^{-1}$ ) = 15.6, 13.5, 11.9, and 18.2 (WT) respectively. The mutations thus show ~ 15 - 35% lower activity than wild-type hGS when measured immediately after (within a few hours) purification (Table 3.2). Wild-type hGS displays negative cooperativity toward its  $\gamma$ -glutamyl substrate ( $\gamma$ -GluABA) with a Hill coefficient of 0.69 (29). The mutant hGS dimer interface enzymes prepared here have nearly identical Hill coefficients (0.68 to 0.72) (Table 3.2). Thus, the three dimer interface residues involved in electrostatic interactions do not significantly impact negative cooperativity in hGS.

The  $\gamma$ -GluABA Michaelis constant ( $K_m$ ), the  $[\gamma\text{-GluABA}]$  where the reaction rate is half of  $V_{\text{max}}$ , and which relates to substrate affinity for the wild-type hGS, of S42A, R221A and D24A are 1.31, 0.95, 0.68 and 0.71 mM, respectively (Table 3.2). Hence, the affinity for  $\gamma$ -GluABA of these dimer interface mutants has increased. Compared to wild-type there is a slight increase in catalytic efficiency ( $k_{\text{cat}}/K_m$ ) of the dimer interface mutants S42A, R221A and D24A (Table 3.2). Therefore, hGS residues (S42, R221 and D24) that have hydrogen bonding and ionic interactions across the dimer interface have a decrease in activity, maintain negative cooperativity, increase in  $\gamma$ -GluABA affinity, and increase in catalytic efficiency when mutated to an alanine.

**TABLE 3.2****Activity, kinetic properties and thermal stability of hGS.**

Enzyme	$k_{cat}$ ( $s^{-1}$ )	$K_m$ (mM)	$k_{cat}/K_m$ ( $s^{-1}M^{-1}$ )	Hill Coef.	$T_m$ ( $^{\circ}C$ )
WT	$18.2 \pm 1.97$ (100%)	$1.31 \pm 0.13$	$1.39 \times 10^4$	$0.69 \pm 0.03$	$60.3 \pm 0.33$ (100%)
S42A	$15.6 \pm 0.50$ (85%)	$0.95 \pm 0.08$	$1.64 \times 10^4$	$0.72 \pm 0.06$	$49.7 \pm 0.07$ (82%)
R221A	$13.5 \pm 2.98$ (74%)	$0.68 \pm 0.08$	$2.00 \times 10^4$	$0.68 \pm 0.04$	$42.5 \pm 0.40$ (70%)
D24A	$11.9 \pm 0.25$ (65%)	$0.71 \pm 0.02$	$1.68 \times 10^4$	$0.68 \pm 0.05$	$39.3 \pm 0.11$ (65%)

Duplicate assays carried out on 2-3 independent purifications (per enzyme).

*Temporal Analysis of Enzyme Activity*-Wild-type hGS is stable for at least 3 years when stored at 4  $^{\circ}C$ ; remarkably, during kinetic studies it was found that over time some hGS mutant enzymes lost activity (rapidly) after purification. More importantly, the change in activity was different for different mutations. For example, within a few hours, both R221A and D24A lost activity in a biphasic manner (Fig. 3.2), *i.e.*, first rapidly and then more gradually. Specifically, D24A lost 30% activity in 4 hours while R221A decreased by 20% in 7.5 hours. In contrast, the S42A hGS enzyme was fairly stable, with only a 10% loss after 3 days, and a 40% loss in activity after 6 weeks (data not shown). Hence, all three of the dimer hGS mutant enzymes decrease in activity over time, with R221A and D24A losing the most activity with respect to time. What is particularly intriguing is that despite the biphasic nature of the loss of activity, both R221A and D24A plateaued at more or less the same  $k_{cat}$  ( $8 s^{-1}$ ), albeit starting from different initial activities.

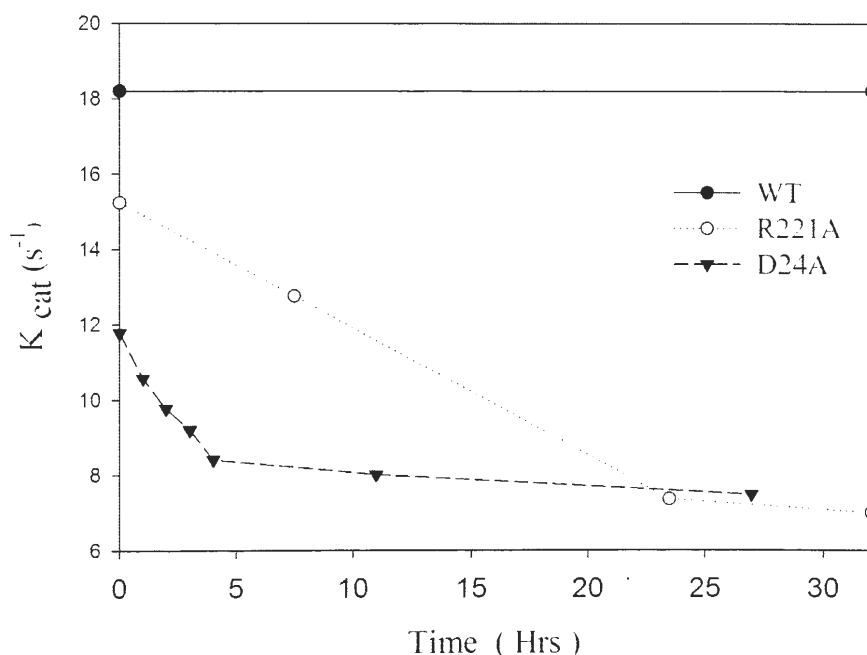


**FIGURE 3.2. Activity of wild-type and hGS mutant enzymes R221A and D24A over time.** Values represent an average of two assays of at least two independent purifications (per enzyme).

*Experimental Measurement of Stability*-Differential scanning calorimetry was used to compare enzyme stability. Wild-type hGS has an unfolding or transition midpoint ( $T_m$ ) of 60.3 °C. The  $T_m$  values of S42A, R221A and D24A are 49.7, 42.5 and 39.3 °C, respectively (Table 3.2). The stability of each hGS mutant enzyme decreased compared to wild-type, supporting the predictions of their importance from the conservation and structural analyses (*vide supra*).

*Circular Dichroism, Secondary Structural Study*-The wild-type hGS circular dichroism (CD) spectrum shows distinct negative bands of molar ellipticity around 212

and 225 nm. The S42A and R221A mutant hGS enzymes have only a slight change in CD spectra. CD spectrum of D24A shows the largest loss of negative molar ellipticity, around 208 nm (Fig S2).

*RMSD Analysis of Molecular Dynamics Geometries*-The structural alignment of S42A, R221A and D24A with wild-type hGS (all are the lowest-energy structures obtained from MD simulations) resulted in an average the root mean square deviation (RMSD) of 1.24, 1.88 and 1.25 Å, respectively; see Table S2, Supplemental Materials for details. Within the dimer region, the RMSD of the three mutants were 1.13 (S42A), 1.60 (R221A) and 1.01 (D24A) Å. Although the D24A and S42A mutants showed similar movement within the protein as a whole, the S42A mutation had a larger impact on the dimer region geometry than the other two hGS dimer interface mutants studied here. Of the mutants studied, R221A had the largest overall RMSD and the largest movement within the dimer region, indicating a significant conformational change.

*Hydrogen Bond Analysis of Molecular Dynamics Geometries*-A summary of all bonds within 4.5 Å of S42, R221 and D24 within the wild-type and mutant hGS enzymes is given in Table S3; the two subunits are designated “a” and “b.” In the wild-type there are two interchain ionic hydrogen bonds and an interchain salt bridge between D24 and R221, two interchain ionic hydrogen bonds between D24 and S42, and one interchain ionic hydrogen bond between E43b and S46a. A comprehensive list of other intrachain interactions is given in Table S3.

Intrachain bonding is largely unaffected by the D24A mutation, Table S3 and Fig. 3.3. (Similar plots for S42A and R221A are given in Figures S3 and S4 within Supplemental Materials.) When D24 is mutated to an alanine, two symmetrical interchain hydrogen bonds between residues E43 and S46 remain but all of the other surrounding interchain hydrogen bonds are disrupted.

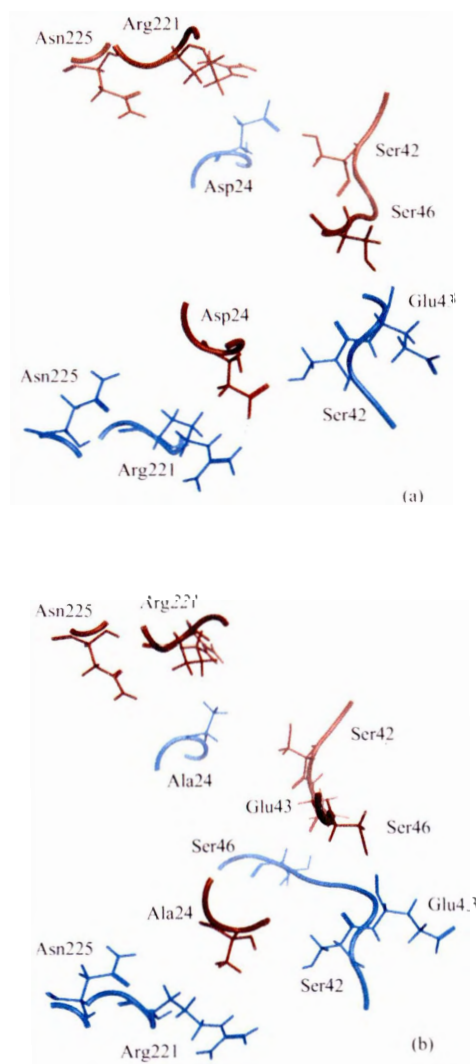


**FIGURE 3.3. Hydrogen bonding in (a) wild-type hGS and (b) D24A hGS.** Chain A is in red (dark) and chain B is in blue (light)

The S42A mutation has an impact on the hydrogen bonding structure of the dimer region. A salt bridge (D24-R34) and an interchain hydrogen bond (S46-A42) form in the S42A mutant in place of the S42-D24, S42-E43 interchain bonds of the wild-type enzyme, Fig. S3. Although the mutation of S42A disrupts some interactions, it also creates new interchain hydrogen bonds (Table S3, Fig. S3), which is consistent with the modest reduction in activity of the S42A enzyme.

Mutation of R221 to alanine disrupts several hydrogen bonds within the dimer region. As expected, the interchain salt bridge, and hydrogen bonds between R221 and D24 are broken. A new salt bridge forms between R34 and D42. The mutation of R221A has a large impact on the intrachain bonding structure (Table S3, Fig S4). Overall, the R221A mutation results in a moderate loss of interchain bonds, when compared with the dramatic drop in interchain bonds in the D24A mutant and the small shift in interchain bonds in the S42A mutant, Table S3.

## **DISCUSSION**

An experimental and computational analysis is reported of three charged or polar amino acid residues at the dimer interface of human glutathione synthetase – S42, R221 and D24 – and their corresponding subunit:subunit interactions. We initially hypothesized that these residues stabilize this homodimeric enzyme and affect the allostery of hGS. To probe these hypotheses, these residues were mutated to alanine (S42A, R221A and D24A) and the impact on activity, stability and allostery of hGS was



measured. Several important conclusions relevant to hGS biochemistry and protein allostery are discussed.

The changes in circular dichroism spectra of the hGS mutant dimer enzymes compared to wild-type hGS suggest a conformational change in structure that is mirrored by changes in thermal stability especially in D24A. The impact of S42A, R221A and D24A on experimental thermal stability ( $T_m$ , Table 2) of hGS is also supported by a computational analysis of interchain hydrogen bonds and salt bridges (Table S3 and Fig. 3). Molecular dynamics studies indicate that mutation of each individual residue to alanine results in modest conformational changes (Table S2), globally as well as locally at the dimer interface. However, these mutations disrupt strong ionic hydrogen bonds and salt bridges across the dimer interface, Fig. 3. Experiment and modeling suggest that D24 has the largest impact on the dimer interface of hGS, followed by R221 and then S42, and further that subunit:subunit interactions involving S42, R221 and D24 are essential to the stability of dimeric hGS.

Decreases in activity and stability of the three hGS mutations show a correlation with the number and strength of subunit:subunit bonds that each residue participates in (i.e.,  $D24 > R221 > S42$ ), Fig. 1 and Fig. 3. To wit, D24A (least active mutant) loses two strong interchain interactions with S42 and R221 in the wild-type hGS. The R221A and S42A mutations each abolish a single strong interaction:  $R221 \cdots D24$  (salt bridge) and  $S42 \cdots D24$  (ionic hydrogen bond). Temporal activity analysis (Fig. 2) of the hGS mutant enzymes further supports the importance of number and strength of interactions. D24A

and R221A each having a rapid decrease in activity, while S42A has a slow decrease in activity. Thus, D24 with its two interactions plays a more pivotal role in hGS activity and stability than the other two residues studied here.

By interrogating these residues via site-directed mutagenesis experiments, it is clear that the dimer interface residues S42, R221 and D24 also affect the Michaelis constant of hGS. The decrease in  $K_m$  for  $\gamma$ -GluABA upon mutation of these residues indicates that the dimer interface residues have a long distance impact on the active site of hGS ( $>11$  Å, based on distances between the C $^\circ$  of the three residues and the C $^\circ$  of the Glu component of  $\gamma$ -Glu substrate in the crystal structure (28)). The experimentally measured increase in binding affinity (decreased  $K_m$ , Table 2) of the  $\gamma$ -GluABA substrate for the three hGS mutant enzymes may explain the drop in activity of the S42A, R221A and D24A mutants. Additionally, reduced enzyme stability may lessen hGS activity to some extent, especially for D24A. Most importantly, cooperativity studies for the  $\gamma$ -GluABA substrate show that their Hill coefficients remain as negatively cooperative as wild-type hGS. Therefore, we must conclude that S42, R221 and D24 are not located on the allosteric pathway of human glutathione synthetase.

There has been substantial discourse (30-34) on the role of strong salt bridges and hydrogen bonds in the context of protein:protein interactions. Despite the passage of more than a century since the first experimental evidence of protein cooperativity, the atomic-level sequence of events that elucidate allostery remains a subject of considerable, if not growing, interest due to recent research in exploiting allostery in new drug

development (1-5,35-47). The residues S42, R221 and D24 form strong, interchain salt bridges and ionic hydrogen bonds and are integral to the stability of hGS. Indeed, the present research in conjunction with previous studies of other dimer interface residues – V44/45 (22) – infers that hGS is an obligate dimer. The negligible changes in Hill coefficient reported here indicate that S42, R221 and D24 do not lie along the allosteric pathway of this negatively cooperative enzyme. In conclusion, the present research on homodimeric hGS implies that strong chemical interactions are essential for the stability of multimeric enzymes, but need not necessarily mediate allosteric communication. Alternatively, one may hypothesize that weaker chemical bonding phenomena, *e.g.*, hydrophobic interactions (22), may provide a more flexible (chemically and evolutionarily) communication pathway between enzyme active sites. By extension, allosteric pathways in enzymes may arise not from a few strong chemical bonds but rather a “conspiracy” among larger numbers of weaker interactions. To this end, studies are underway in our laboratory to further delineate the allosteric pathways and protein:protein interactions of hGS, which may shed light on this cooperative ATP-grasp enzyme, as well as provide the essential data needed to test the various models of protein allostery.

*Acknowledgements*-The authors thank the Chemical Computing Group for providing the MOE software. We also thank Amy Graves, Teresa Brown, and Sarah Barelier for technical assistance and Mark Britt and Richard Sheardy for instrumentation assistance.

## **FOOTNOTES**

Supported in part by NIH R15GM086833 (MEA), a Research Enhancement Program Grant (TWU, MEA), and a UNT Faculty Research Grant (TRC).

## REFERENCES

1. Haber, J.E., and Koshland D.E., Jr. (1967) Relation of protein subunit interactions to the molecular species observed during cooperative binding of ligands. *Proc. Natl. Acad. Sci. USA*. **58**, 2087-2093
2. Kirtley, M.E., and Koshland, D.E., Jr. (1967) Models for cooperative effects in proteins containing subunits. Effects of two interacting ligands. *J. Biol. Chem.* **242**, 4192-4205
3. Adair, G.S. (1925) The hemoglobin system. VI. The oxygen dissociation curve of hemoglobin. *J. Biol. Chem.* **63**, 529-545
4. LiCata, V.J., and Allewell, N.M. (1998) Solvent perturbation of the allosteric regulation of aspartate transcarbamylase. *Biochim. Biophys. Acta*. **1384**, 306-314
5. Kantrowitz, E.R. (2012) Allostery and cooperativity in Escherichia coli aspartate transcarbamoylase. *Arch. Biochem. Biophys.* **519**, 81-90
6. Geitmann, M., Elinder, M., Seeger, C., Brandt, P., de Esch, I.W.J., and Danielson, U.H. (2011) Identification of a novel scaffold for allosteric inhibition of wild type and drug resistant HIV-1 reverse transcriptase by fragment library screening. *J. Med. Chem.* **54**, 699-708
7. Wells, J.A., McClendon, C.L. (2007) Reaching for high hanging fruit in drug discovery at protein-protein interfaces. *Nature*. **450**, 1001-1009
8. Calleja, V., Laguerre, M., and Larijani, B. (2009) 3-D structure and dynamics of protein kinase B-new mechanism for the allosteric regulation of an AGC kinase. *J. Chem. Biol.* **2**, 11-25
9. Kalodimos, C.G. (2012) Protein function and allostery: a dynamic relationship. *Ann. N.Y. Acad. Sci.* **1260**, 81-86
10. Tzeng, S., Kalodimos, C.G. (2011) Protein dynamics and allostery: an NMR view. *Curr. Opin. Struct. Biol.* **21**, 62-67
11. Meister, A., and Anderson, M. E. (1983) Glutathione. *Annu. Rev. Biochem.* **52**, 711-60
12. Oppenheimer, L., Wellner, V.P., Griffith, O.W., and Meister, A. (1979) Glutathione synthetase purification from rat kidney and mapping of the substrate binding sites. *J. Biol. Chem.* **254**, 5184-5189
13. Ristoff, R., and Larsson, A. (2002) Oxidative stress in inborn errors of metabolism: lessons from glutathione deficiency. *J. Inherit. Metab. Dis.* **25**, 223-226
14. Bains, J.S., and Shaw, C.A. (1997) Neurodegenerative disorders in humans: the role of glutathione in oxidative stress-mediated neuronal death. *Brain Res. Rev.* **25**, 335-358
15. Larsson, A., Ristoff, E., and Anderson, M.E., Glutathione synthetase deficiency and other disorders of the  $\gamma$ -glutamyl cycle (2005) *In* Metabolic Basis of Inherited Disease, Online (genetics.accessmedicine.com) (Scriver, C.R., Beaudet, A.L., Sly, W.S., and Valle, D., Eds.) McGraw Hill, New York

16. Townsend, D.M., Tew, K.D., and Tapiero, H. (2003) The importance of glutathione in human disease. *Biomed. Pharmacother.* **57**, 145-155
17. Galperin, M.Y., and Koonin, E.V. (1997) A diverse superfamily of enzymes with ATP-dependent carboxylate-amine/thiol ligase activity. *Protein Sci.* **6**, 2639-2643
18. Meister, A. (1974). Glutathione synthesis. *In* The Enzymes (P. D. Boyer, Ed.), pp. 671–697. Academic Press, New York
19. Jez, J. M., and Cahoon, R.E. (2004) Kinetic Mechanism of Glutathione Synthetase from *Arabidopsis thaliana*. *J. Biol. Chem.* **279**, 42726-42731
20. Galperin, M.Y., and Koonin, E.V. (2012) Divergence and convergence in enzyme evolution. *J. Biol. Chem.* **287**, 21-28
21. Fawaz, M.V., Topper, M.E., and Firestone, S.M. (2011) The ATP-grasp enzymes. *Bioorg. Chem.* **39**, 185-191
22. Slavens, K.D., Brown, T.R., Barakat, K.A., Cundari, T.R., and Anderson, M.E. (2011) Valine 44 and valine 45 of human glutathione synthetase are key for subunit stability and negative cooperativity. *Biochem. Biophys. Res. Commun.* **410**, 597-601
23. Dinescu, A., Cundari, T.R., Bhansali, V.S., Luo, J.L., and Anderson, M.E. (2004) Function of conserved residues of human glutathione synthetase. *J. Biol. Chem.* **279**, 22412–22421
24. Dinescu, A., Brown, T.R., Barelier, S., Cundari, T.R., and Anderson, M.E. (2010) The role of the glycine triad in human glutathione synthetase. *Biochem. Biophys. Res. Commun.* **400**, 511-516
25. Brown, T. R., Drummond, M. L., Barelier, S., Crutchfield, A. S., Dinescu, A., Slavens, K. D., Cundari, T. R., and Anderson, M. E. (2011) Aspartate 458 of human glutathione synthetase is important for cooperativity and active site structure. *Biochem. Biophys. Res. Comm.* **411**, 536-542
26. Lowry, O.H., Rosebrough, N.J., Farr, A.L., and Randall, R.J. (1951) Protein measurement with the folin phenol reagent. *J. Biol. Chem.* **193**, 265–275
27. Dinescu, A., Anderson, M.E., and Cundari, T.R. (2007) Catalytic loop motion in human glutathione synthetase: a molecular modeling approach. *Biochem. Biophys. Res. Commun.* **353**, 450-456
28. Polekhina, G., Board, P.G., Gali, R.R., Rossjohn, J., and Parker, M.W. (1999) Molecular basis of glutathione synthetase deficiency and a rare gene permutation event. *EMBO J.* **12**, 3204-3213
29. Luo, J.L., Huang, C.S., Babaoglu, K., and Anderson, M.E. (2000) Novel kinetics of mammalian glutathione synthetase: characterization of gamma-glutamyl substrate cooperative binding. *Biochem. Biophys. Res. Commun.* **275**, 577–581
30. Jones, S., and Thornton, J.M. (1995) Protein-protein interactions: a review of protein dimer structures. *Prog. Biophys. Molec. Bio.* **63**, 31-65
31. Jones, S., and Thornton, J.,M. (1996) Principles of protein-protein interactions. *Pro. Natl. Acad. Sci. USA.* **93**, 13-20
32. Xu, D., Tsai, C., and Nussinov, R. (1997) Hydrogen bonds and salt bridges across protein-protein interfaces. *Protein Eng.* **10**, 999-1012

33. Keskin, O., Gursoy, A., Ma, B., and Nussinov, R. (2008) Principles of protein-protein interactions: what are the preferred ways for proteins to interact? *Chem. Rev.* **108**, 1225-1244
34. Hendsch, S.Z. and Tidor, B. (1994) Do salt bridges stabilize proteins? A continuum electrostatic analysis. *Protein Sci.* **3**, 211-226
35. Bohr, C., Hasselbach, K.A., and Krogh A. (1904) *Skand. Arch. Physiol.* **16**, 402 – 412 quoted in Koshland, D.E., Jr., and Hamadani, K. (2002) Proteomics and models for enzyme cooperativity. *J. Biol. Chem.* **277**, 46841-46844
36. Ruzicka, F.J., and Frey, P.A. (2010) Kinetic and spectroscopic evidence of negative cooperativity in the action of lysine 2,3-aminomutase. *J. Phy. Chem. B* **114**, 16118-24
37. Urwyler, S., and Sibley, D.R. (2011) Allosteric modulation of family C G-protein coupled receptors: from molecular insights to therapeutic perspectives. *Pharmacol. Rev.* **63**, 59-126
38. Zhuravlev, P.I., and Papoian, G.A. (2010) Protein functional landscapes, dynamics, allostery: a tortuous path towards a universal theoretical framework. *Quart. Rev. Biophys.* **43**, 295-332
39. Rader, A.J., and Brown, S.M. (2011) Correlating allostery with rigidity. *Mol. Biosyst.* **7**, 464-471
40. Min, W., Jiang, L., and Xie, X.S. (2010) Complex kinetics of fluctuating enzymes: phase diagram characterization of a minimal kinetic scheme. *Chem. Asian J.* **5**, 1129-1138
41. Nieland, T.J.F., Xu, S., Penman, M., and Krieger, M. (2011) Negatively cooperative binding of high-density lipoprotein to the HDL receptor SR-BI. *Biochemistry* **50**, 1818-1830
42. Goodey, N., and Benkovic, S.J. (2008) Allosteric regulation and catalysis emerge via a common route. *Nature Chem. Bio.* **4**, 474-482
43. Cui, Q., and Karplus, M. (2008) Allostery and cooperativity revisited. *Protein Sci.* **17**, 1295-307
44. Swain, J.F., and Gierasch, L.M. (2006) The changing landscape of protein allostery. *Curr. Opp. Struct. Bio.* **16**, 102-108
45. Koshland, D.E., Jr. (1996) The structural basis of negative cooperativity: receptors and enzymes. *Curr. Opin. Struct. Biol.* **6**, 757-61
46. Yu, E.W., and Koshland, D.E., Jr. (2001) Propagating conformational changes over long (and short) distances in proteins. *Proc. Natl. Acad. Sci. USA.* **98**, 9517-9520
47. Gutheil, W.G. (1992) Thermodynamic model of cooperativity in a dimeric protein: unique and independent parameters formulation. *Biophys. Chem.* **45**, 181-191

## SUPPLEMENTAL MATERIALS

The following supplemental materials include computational methods and references, tables for the mutant enzyme primers, RMSD analysis, and hydrogen bond analysis, as well as figures of hGS, the circular dichroism spectra of the dimer interface mutant enzymes and WT, and the hydrogen bonding seen in mutant enzymes S42A and R221A.

## COMPUTATIONAL METHODS

*Structural Analysis of hGS*-The crystallographic coordinates of dimeric hGS (product form, PDB code = 2HGS (28) were analyzed. Interchain protein-contacts within the dimer region of the wild-type hGS crystal structure were determined. Contact types (hydrogen bonds, hydrophobic contacts, *etc.*) and pertinent atomic distances were computed with the MOE program (48).

*Sequence Analysis*-Utilizing the NCBI database, the sequence of hGS (2HGS) was matched to known protein sequences using BLAST and a non-redundant database and aligned using the BLOSUM62 matrix (49-51). Hypothetical and theoretical sequences were eliminated from the alignment. Conservation was determined for all higher eukaryote and all mammalian sequences. Percent conservation of each residue was calculated relative to wild-type hGS. Percent charge conservation at each site was also calculated assuming biological pH of 7.6. Aspartic and glutamic acid side chains were assumed to be negatively charged, while arginine and lysine were treated as positively charged. All other amino acids were considered neutral.



*Ab Initio Calculation of Amino Acid Interactions*-The GaussView (52) program was used to construct models of interacting residue pairs found at the dimer interface of hGS. A search was performed using MOE (48) and the Amber99 force field (53) to find the lowest energy conformer, which was subsequently refined with *ab initio* calculations using the GAMESS (54) program with density functional theory (B3LYP/6-31+G(d)) (55-57) both in the gas phase and in aqueous solution (57). Interacting amino acid pairs were analyzed in the absence of the surrounding amino acids and the residues are truncated at the alpha carbon, which was replaced by a methyl group. For the latter, the polarizable continuum model (PCM) was employed to compute solvent effects (58).

*Molecular Dynamics Simulations*-Using MOE (48), waters and substrates were removed from 2HGS (28). The resulting file was used as input for molecular dynamics (MD) simulations in GROMACS 4.5.5 (59-61). The AMBER99 force field was used for all calculations (53). Within GROMACS, H atoms were added to the enzyme, which was placed in a dodecahedral box with borders of 1.0 Å. The box was solvated using the simple point charge water model (62). The charge was neutralized with randomly dispersed Na<sup>+</sup> and Cl<sup>-</sup> to a concentration of 0.15 M. An initial geometry optimization was conducted in GROMACS with the structure converging with forces  $\leq 10 \text{ kJ mol}^{-1} \text{ nm}^{-1}$ . Finally, an unconstrained molecular dynamics run was conducted. The temperature increased from 0 to 300 K over a 1 ps interval. The wild-type hGS MD simulation ran for 8 ns in 0.5 fs time steps with data saved every 0.5 ps. The Particle Mesh Ewald method was used for long range electrostatic interactions (59). Mutant hGS enzymes were

simulated using the same method with the variation that simulations were run for 1 ns with 0.5 fs time steps.

The lowest energy conformation from the wild-type hGS MD run was extracted and used as the starting structure for mutants. For each mutant, the relevant residues (S42, R221 and D24) in each chain were mutated to alanine. These structures were then used as inputs for the aforementioned MD run.

*RMSD Calculations*-The three mutants were aligned relative to the wild-type hGS structure using an all atom sequence and structure alignment in MOE (49). The root mean square deviation (RMSD) for each mutant was then collected for the  $\alpha$ -carbons. The average deviation of the chains was taken as the RMSD for each residue.

*Hydrogen Bond Analysis of Molecular Dynamics Structures*-Analysis was conducted on residues of the dimer interface in each low energy structure, comparing the bond lengths and angle of each hydrogen bond to an idealized bond with a length (heavy atom to heavy atom separation) of 3.0 Å and angle of 180°. For the wild-type structure, bonds between all residues within 4.5 Å of S42, R221 and D24 were analyzed. Bonds between these residues and any other bonds within 4.5 Å of the mutation were similarly analyzed for mutants.

48. MOE (Molecular Operating Environment) Chemical Computing Group Inc., <http://www.chemcomp.com>
49. Altschul, S.F., Madden, T.L., Schäffer, A.A., Zhang, J., Zhang, Z., Miller, W., and Lipman, D.J. (1997) Gapped BLAST and PSI-Blast: a new generation of protein database search programs. *Nucleic Acids Res.* **25**, 3389-3402

50. Berman, H.M., Westbrook, J., Feng, Z., Gilliland, G., Bhat, T.N., Weissig, H., Shindyalov, I.N., and Bourne, P.E. (2000) The protein data bank. *Nucleic Acids Res.* **28**, 235-42. ([www.pdb.org](http://www.pdb.org))
51. Meng, E.C., Pettersen, E.F., Couch, G.S., Huang, C.C., and Ferrin, T.E. (2006) Tools for integrated sequence-structure analysis with UCSF Chimera. *BMC Bioinformatics.* **7**, 339
52. [http://www.gaussian.com/g\\_prod/gv5.htm](http://www.gaussian.com/g_prod/gv5.htm)
53. Cornell, W.D., Cieplak, P., Bayly, C.I., Gould, I.R., Merz, K., Ferguson, D.M., Spellmeyer, D.C., Fox, T., Caldwell, J.W., Kollman, P.A. (1995) A second generation force field for simulation of proteins, nucleic acids, and organic molecules. *J. Am. Chem. Soc.* **117**, 5179-5197
54. Schmidt, M.W., Baldridge, K.K., Boatz, J.A., Elbert, S.T., Gordon, M.S., Jensen, J.J., Koseki, S., Matsunaga, N., Nguyen, K.A., Su, S., Windus, T.L., Dupuis, M., and Montgomery, J.A. (1993) General atomic and molecular electronic structure system. *J. Comput. Chem.* **14**, 1347-1363
55. Becke, A. D. (1993) Density-functional thermochemistry. III. The role of exact exchange. *J. Chem. Phys.* **98**, 5648-5652
56. Hehre, W.J., Ditchfield, R., and Pople, J.A. (1972) Self-consistent molecular orbital methods. XII. Further extensions of Gaussian-type basis sets for use in molecular orbital studies of organic molecules. *J. Chem. Phys.* **56**, 2257-2261
57. Francl, M.M., Pietro, W.J., Hehre, W.J., Binkley, J.S., Gordon, M.S., DeFrees, D.J. and Pople, J.A. (1982) A polarization basis set for second row elements. *J. Chem. Phys.* **77**, 3654-3665
58. Tomasi, J., Mennucci, B., and Cammi, R. (2005) Quantum mechanical continuum solvation models. *Chem. Rev.* **105**, 2999-3093
59. Berendsen, H.J.C., van der Spoel, D., and van Drunen, R. (1995) GROMACS: a message-passing parallel molecular dynamics implementation. *Comp. Phys. Comm.* **91**, 43-56
60. Hess, B., Kutzner, C., van der Spoel, D., and Lindahl, E. (2008) GROMACS 4: algorithms for highly efficient, load-balanced, and scalable molecular simulation. *J. Chem. Theory Comput.* **4**, 435-447
61. van der Spoel, D., Lindahl, E., Hess, B., Groenhof, G., Mark, A.E., and Berendsen, H.J.C. (2005) GROMACS: fast, flexible and free. *J. Comput. Chem.* **26**, 1701-1718
62. Berendsen, H., Postma, J., van Gunsteren, W., Hermans, J. Interaction models for water in relation to protein hydration (1981) In *Intermolecular Forces*. (Pullman, B., Ed.), pp 331-38. D. Reidel Publishing Company, Dordrecht, Netherlands.

**TABLE S1**

**Primers for site directed mutagenesis of S42, R221 and D24 of glutathione synthetase.**

<b>Enzyme</b>	<b>DNA Sequence</b>
S42A	5'- GCC CAC TTC <u>CGC</u> AGA GGT GGT GAG C – 3' 5'- GCT CAC CAC CTC <u>TGC</u> GGA AGT GGG C – 3'
R221A	5'- GGA AAG AAA CAT ATT TGA CCA <u>GGC</u> <u>TGC</u> CAT AGA G – 3' 5'- CTC TAT GGC <u>AGC</u> CTG GTC AAA AAT GTT TCT TTC C – 3'
D24A	5'- CAG GCC GTG <u>GCC</u> CGG GCC CTG – 3' 5'- CAG GGC CCG <u>GGC</u> CAC GGC CTG – 3'

Underlined bases are changed nucleotide positions.

**TABLE S2**

**RMSD of hGS mutants relative to wild-type hGS in Å.**

<b>Residue</b>	<b>D24A</b>	<b>S42A</b>	<b>R221A</b>
<b>D24</b>	0.84	0.81	0.93
<b>S42</b>	0.96	1.26	1.58
<b>E43</b>	1.62	1.66	2.45
<b>V44</b>	1.06	1.19	1.54
<b>V45</b>	0.52	0.56	0.99
<b>Y47</b>	0.65	1.01	0.75
<b>R221</b>	0.62	0.41	1.17
<b>Average</b>	1.256	1.244	1.881
<b>St Dev</b>	0.738	0.753	1.211

**TABLE S3**

**Hydrogen bond analysis of wild-type and mutants hGS; bond lengths in Å; bond angles in °.** Table continued on page 38-39.

<b>Wild-type</b>					
	Bonded Atoms		Type	Length	Angle
Interchain Bonds	D24a	S42b	HB	2.66	168.5
	D24a	R221b	SB	3.07	148.7
	D24a	R221b	HB	3.02	154.5
	S42a	D24b	HB	2.69	176.2
	S46a	E43b	HB	2.63	166.8
	R221a	D24b	HB	3.05	143.8
Intrachain Bonds	R34a	S42a	HB	3.03	128.3
	R34a	S42a	SB	2.83	151.7
	E43a	S41a	HB	3.37	161.1
	S46a	Y47a	HB	2.99	131.8
	Q220a	R236a	HB	2.95	162.5
	Q220a	R236a	SB	2.71	138.1
	E224a	R326a	HB	2.63	163.9
	R34b	S42b	HB	2.88	150.0
	R34b	S42b	SB	3.06	134.0
	E43b	S41b	HB	2.56	168.6
	Q220b	R236b	HB	3.07	142.8
	Q220b	R236b	SB	2.71	160.8
	E224b	R236b	HB	2.91	167.7
	E224b	R221b	HB	2.84	149.7
<b>D24A</b>					
	Bonded Atoms		Type	Length	Angle
Interchain Bonds	E43a	S46b	HB	2.85	157.6
	S46a	E43b	HB	2.72	170.8
Intrachain Bonds	R34a	S42a	HB	3.06	170.8
	R221a	E224a	HB	2.74	159.4
	Q220a	R236a	HB	2.77	135.5
	Q220a	R236a	SB	2.79	151.5
	E224a	R236a	HB	2.82	149.5
	R34b	S42b	HB	3.13	137.5
	R34b	S42b	HB	3.03	155.5
	S41b	E43b	HB	3.43	169.9
	S41b	E43b	HB	2.65	142.0
	Q220b	R236b	HB	2.93	148.2

	Q220b	R236b	SB	2.83	159.0
	R221b	E224b	HB	2.94	160.7
	E224b	R236b	HB	2.79	149.6

#### S42A

	Bonded Atoms		Type	Length	Angle
Interchain Bonds	D24a	R221b	SB	2.80	139.3
	D24a	R221b	HB	2.72	154.5
	R34a	D24b	SB	2.96	159.1
	S46a	A42b	HB	2.74	124.0
	R221a	D24b	HB	2.78	156.3
	R221a	D24b	SB	2.76	154.4
Intrachain Bonds	T40a	T40a	HB	2.64	119.0
	S46a	Y47a	HB	2.76	130.5
	Q220a	R236a	HB	2.80	144.9
	Q220a	R236a	SB	2.91	139.4
	R221a	E224a	HB	2.70	169.7
	E224a	R236a	HB	2.85	143.5
	Q220b	R236b	HB	2.99	154.7
	Q220b	R236b	SB	2.95	146.0
	R221b	E224b	HB	3.00	169.7

#### R221A

	Bonded Atoms		Type	Length	Angle
Interchain Bonds	D24a	S42b	HB	2.67	160.2
	R34a	D42b	SB	2.75	147.0
	S42a	D24b	HB	2.48	157.0
	S46a	E43b	HB	2.95	160.5
Intrachain Bonds	Q220a	R236a	HB	2.91	135.0
	Q220a	R236a	SB	2.92	149.5
	E224a	R236a	HB	2.83	162.2
	Q220b	R236b	HB	2.73	159.0
	Q220b	R236b	SB	2.83	136.2
	E224b	R236b	HB	2.83	157.6

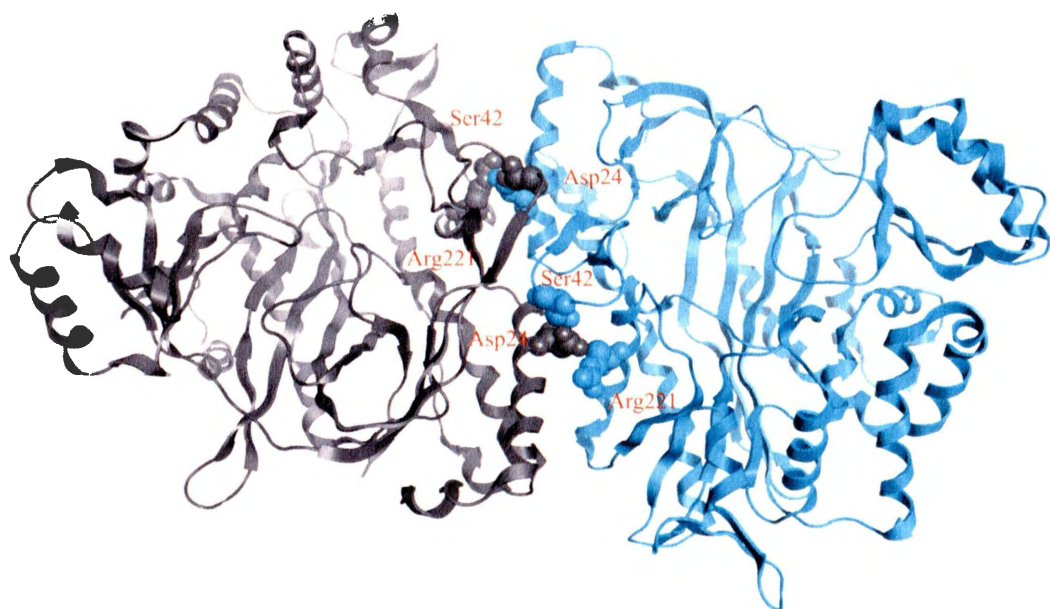
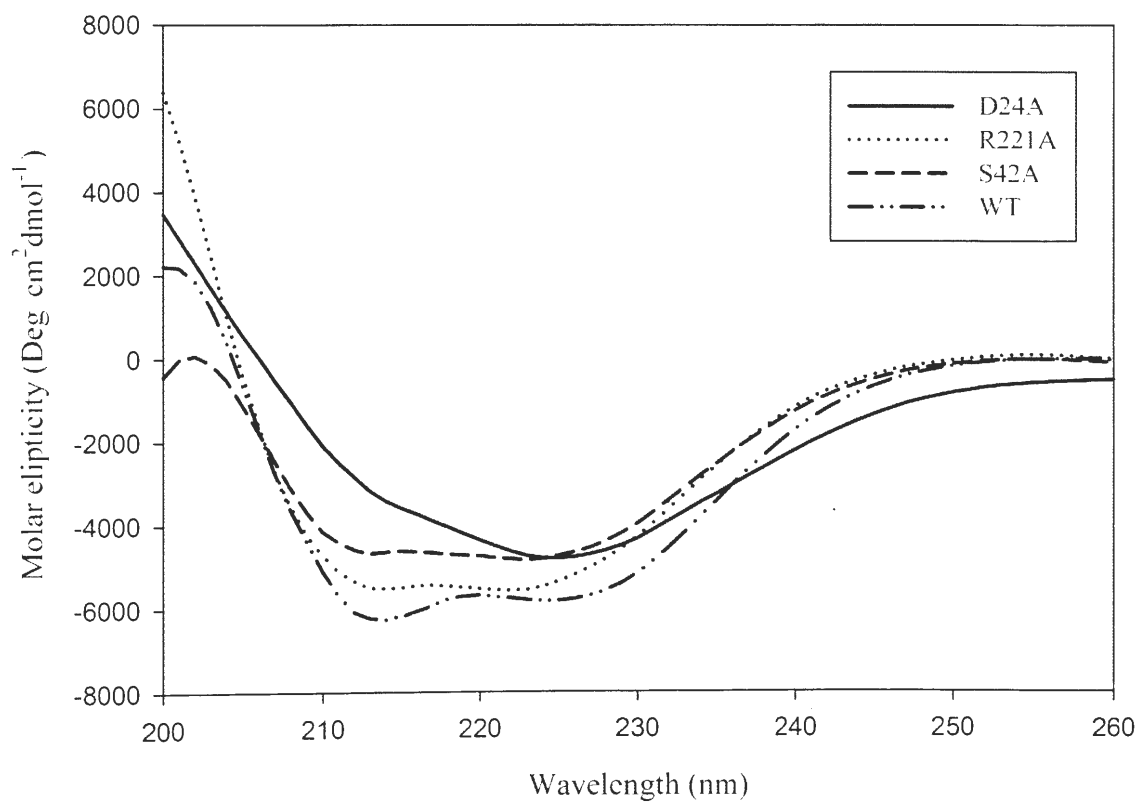


FIGURE S1. **Homodimeric human glutathione synthetase.** Chain A (gray ribbon), chain B (cyan ribbon); residues S42, R221 and D24 are shown in a space-filling representation.



**FIGURE S2. Circular dichroism spectra of wild-type hGS and dimer interface hGS mutant enzymes (S42A, R221A and D24A).**



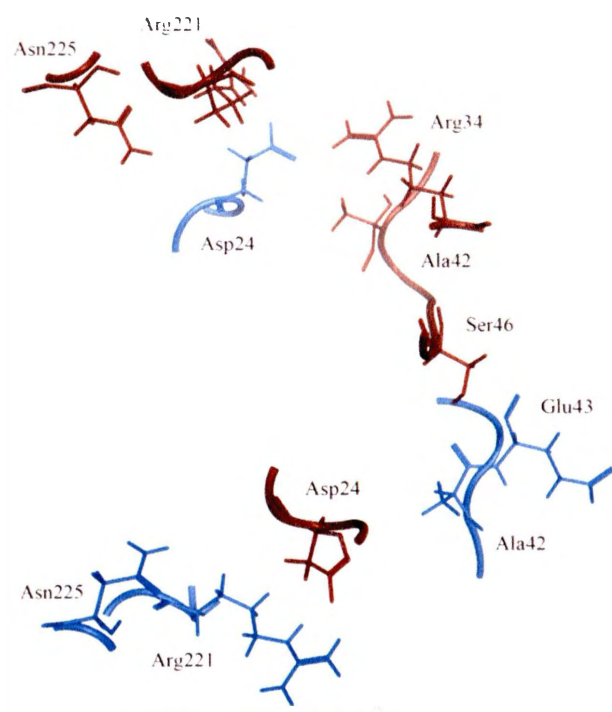


FIGURE S3. **Hydrogen bonding in S42A mutant hGS.** Chain A is in red (dark) and chain B is in blue (light).

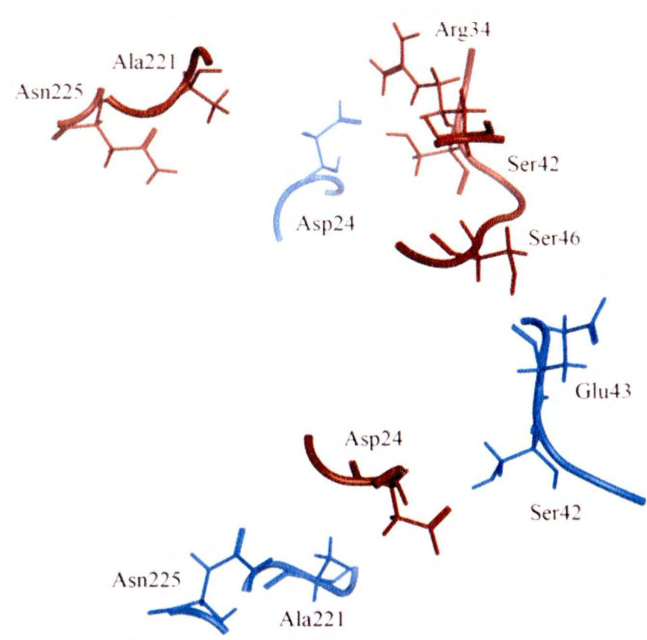


FIGURE S4. **Hydrogen bonding in R221A mutant hGS.** Chain A is in red (dark) and chain B is in blue (light).

## CHAPTER IV

### PROPERTIES OF THE DIMER LOOP OF HUMAN GLUTATHIONE SYNTHETASE

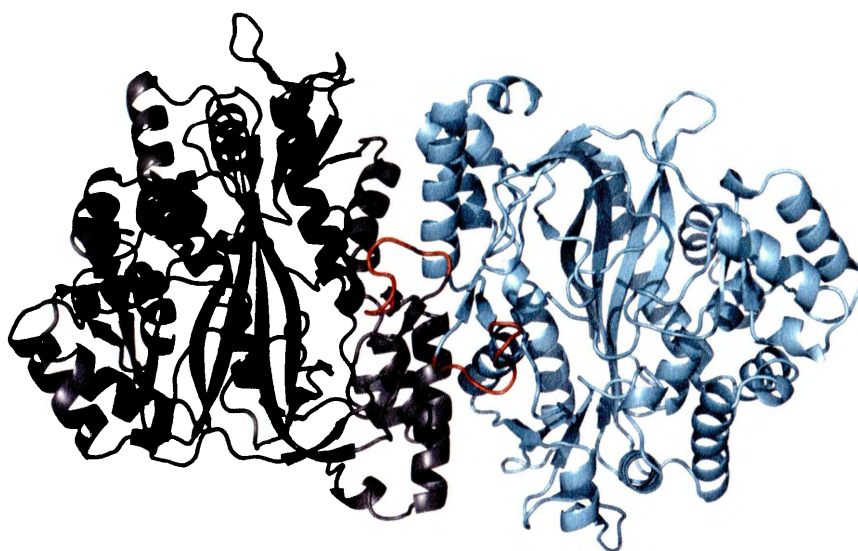


FIGURE 4.1. **The dimer loop (red) of hGS.** Chain A (gray ribbon), chain B (cyan ribbon).

#### INTRODUCTION

The dimer loop [35-TSQEPTSSE-43] (fig 4.1 and 4.2) is located at the dimer interface of hGS. Based on the location of the loop, it is hypothesized that the loop or residues within the loop may play a role in the allostery of hGS. Based on sequence

conservation analysis (next section) and computational studies, focus was placed on residues Thr35, Ser36, Pro39, Ser41, Ser42, and Glu43. Alanine mutations of each of the aforementioned residues were prepared, purified, and analyzed for changes in cooperativity, activity, and thermal stability.

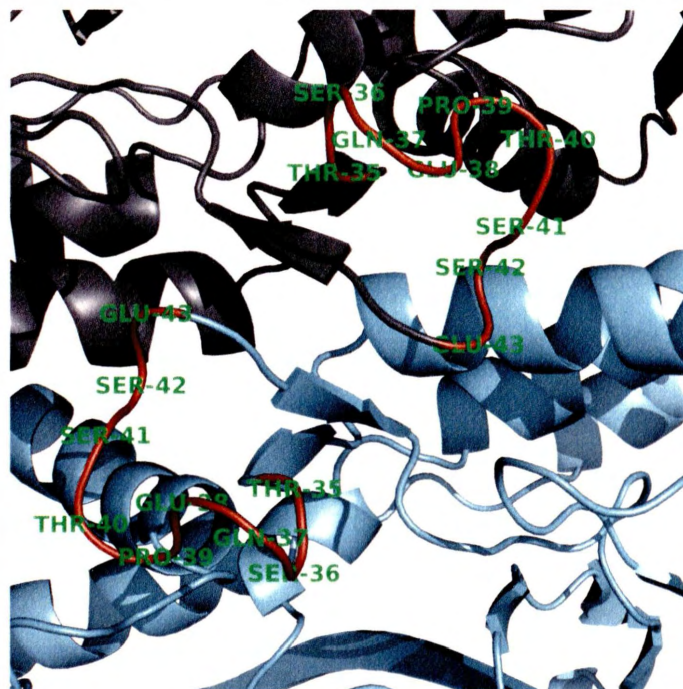


FIGURE 4.2. Close-up view of the dimer loop (red) of hGS.

## METHODS

See chapter II methodology, page 5.

## RESULTS

*Sequence Conservation*-Sequence analysis of hGS with glutathione synthetase of higher eukaryotes (prokaryotes display significantly greater sequence variability, data not

shown) showed an average conservation of 43% and an average charge conservation of 60%. Among mammals, the average conservation of all amino acids in hGS is 71% (average charge conservation: 76%), Table 4.1. Conservation and charge conservation among the dimer loop in higher eukaryotes is not high (Table 4.1), with only residue S41 (47.6%) above the average conservation of amino acid residues relative to hGS, and P39A (62.2%) and S41A (67.1%) above the average charge conservation of amino acid residues relative to hGS. Conservation of dimer loop residues increased when only comparing mammal species of GS (residues P39A (61.9%), S41 (61.9%), and S42 (61.9%)). Charge conservation for dimer loop residues in mammals is high in residues T35 (61.9%), S36 (66.7%), P39A (76.2%), T40 (71.4%), S41A (76.2%) and S42 (66.7%) when compared to all amino acid residues relative to hGS. A high charge conservation of the dimer loop among mammals suggests evolutionary importance of residues in mammals.

**TABLE 4.1**

**Comparison of the conservation of hGS dimer loop residues between higher eukaryotes and mammals.**

<b>Residue</b>	<b>Higher Eukaryotes*</b>		<b>Mammals</b>	
	<b>%C</b>	<b>%CC</b>	<b>%C</b>	<b>%CC</b>
<b>T35</b>	14.6	29.3	42.9	61.9
<b>S36</b>	20.7	40.2	42.9	66.7
<b>Q37</b>	12.2	50.0	47.6	47.6
<b>E38</b>	12.2	14.6	33.3	33.3
<b>P39</b>	26.8	62.2	61.9	76.2
<b>T40</b>	7.3	36.6	23.8	71.4
<b>S41</b>	47.6	67.1	61.9	76.2
<b>S42</b>	24.4	59.8	61.9	66.7
<b>E43</b>	7.3	14.6	23.8	52.4
<b>Average</b>	42.6	60.3	70.5	76.0
<b>St Dev</b>	18.2	19.8	17.3	11.2

\*Higher eukaryotes include species from the Plantae and Animalia kingdoms; %C = conservation; %CC = charge conservation (positive, negative or neutral); Ave = average conservation for all amino acids relative to hGS. St Dev = sample standard deviation.

*Activity and Kinetic Studies of hGS Mutant Enzymes-* The activity of wild-type hGS has a  $k_{\text{cat}} = 19.3 \text{ s}^{-1}$ . The dimer loop mutant hGS enzymes T35A, S36A, P39A, S41A, S42A and E43A have  $k_{\text{cat}} = 16.0, 15.1, 13.4, 14.1, 15.6$  and  $16.2 \text{ s}^{-1}$ , respectively (~ 11 - 26% lower activity than wild-type), when measured within a few hours of purification (Table 4.2). Temporal activity on dimer loop mutant enzymes collected over weeks and then months after enzyme purification show a slow decrease in activity over time (data not shown).

Wild-type hGS displays negative cooperativity toward its  $\gamma$ -glutamyl substrate ( $\gamma$ -GluABA) with a Hill coefficient of 0.69 (Luo, Huang, Babaoglu, & Anderson, 2000). All

dimer loop mutant enzymes have Hill coefficients comparable to wild-type except E43A, which has a slight decrease in negative cooperativity (Table 4.2). Thus, mutation of the dimer loop residues does not significantly impact the allostery of hGS.

The  $\gamma$ -GluABA Michaelis values ( $K_m$ ), which relates to substrate affinity, for the wild-type hGS, T35A, S36A, P39A, S41A, S42A, and E43A are 1.31, 1.40, 1.59, 0.91, 1.64, 0.95 and 1.42 mM, respectively (Table 4.2). The affinity for  $\gamma$ -GluABA increased for hGS mutant enzymes S36A and S41A, decreased for mutant enzymes S42A, and P39A, and remained the same for the remaining dimer loop mutant enzymes when compared to wild-type. Compared to wild-type mutant hGS enzymes T35A, S36A, S41A, and E43A have a slight decrease in catalytic efficiency and mutant hGS enzymes P39A and S42A have a slight increase in catalytic efficiency ( $k_{cat}/K_m$ ) (Table 4.2). Therefore, hGS residues (T35A, S36A, P39A, S41A, S42 and E43A) which are located near/within the dimer interface, have a decrease in activity, maintain negative cooperativity, and have changes in  $\gamma$ -GluABA affinity and catalytic efficiency when mutated to an alanine.

**TABLE 4.2****Activity, kinetic properties and thermal stability of hGS enzymes.**

Enzyme	$k_{cat}$ ( $s^{-1}$ )	$K_m$ (mM)	$k_{cat}/K_m$ ( $s^{-1}M^{-1}$ )	Hill Coef.	$T_m$ (K)
WT	$18.2 \pm 1.97$ (100%)	$1.31 \pm 0.13$	$1.39 \times 10^4$	$0.69 \pm 0.03$	$333.4 \pm 0.33$
T35A	$16.0 \pm 0.28$ (88%)	$1.40 \pm 0.52$	$1.14 \times 10^4$	$0.68 \pm 0.04$	$326.2 \pm 0.04$
S36A	$15.1 \pm 1.02$ (83%)	$1.59 \pm 0.14$	$9.50 \times 10^3$	$0.76 \pm 0.09$	$337.2 \pm 0.05$
P39A	$13.4 \pm 1.20$ (74%)	$0.91 \pm 0.26$	$1.47 \times 10^4$	$0.66 \pm 0.03$	$324.8 \pm 0.21$
S41A	$14.1 \pm 1.17$ (77%)	$1.64 \pm 0.35$	$8.60 \times 10^3$	$0.69 \pm 0.02$	$328.6 \pm 0.32$
S42A	$15.6 \pm 0.49$ (86%)	$0.95 \pm 0.06$	$1.64 \times 10^4$	$0.72 \pm 0.04$	$322.8 \pm 0.07$
E43A	$16.2 \pm 0.71$ (89%)	$1.42 \pm 0.35$	$1.14 \times 10^4$	$0.83 \pm 0.03$	$328.8 \pm 0.07$

Duplicate assays carried out on 2-3 independent purifications (per enzyme).

*Experimental Measurement of Stability*-Differential scanning calorimetry was carried out to compare enzyme stability. Wild-type has a transition midpoint ( $T_m$ ) of 60.3°C. The  $T_m$  of T35A, S36A, P39A, S41A, S42A and E43A are 53.1°C, 64.0°C; 51.7°C, 55.5°C, 49.7°C and 55.6°C, respectively (Table 4.2). The majority of the dimer loop mutant enzymes decreased in  $T_m$ . Dimer loop mutant S36A increased in  $T_m$  ( $\Delta 4$ ). The stability of each hGS mutant enzyme has been altered, with the majority of the dimer loop mutant enzymes decreasing in stability and S36A increasing in stability, compared to wild-type.

## DISCUSSION

An experimental analysis and conservation study of the dimer loop residues (T35, S36, P39, S41, S42, and E43) that are located at the dimer interface of human glutathione synthetase is reported here. We initially hypothesized that these residues affect the



allostery of hGS. To probe this hypotheses, these residues were mutated to alanine (T35A, S36A, P39A, S41A, S42A and E43A) and the impact on activity, stability and allostery of hGS was measured. Several conclusions relevant to hGS biochemistry and protein allostery are discussed.

Overall sequence conservation of the dimer loop is not high, which can be attributed to the fact that not all species of GS are homodimers. The sequence analysis does show that residues P39 and S41 have an above average charge conservation among mammals indicating the importance of charge for those positions in the dimer loop of hGS.

When comparing the activity loss and the decrease in thermal stability of the dimer mutant enzymes, P39A has a significant comparable decrease in both hGS activity (down 26%) and thermal stability compared to wild-type. The drop in activity and thermal stability may be attributed to the structure loss in the dimer loop from mutating the proline to an alanine

Activity loss of the other dimer loop mutant enzymes ranges from 11% (E43A) to 23% (S41A). Residues P39 and S41 had the largest drop in activity when changed to an alanine, which could be attributed back to the importance in conservation they have in the dimer loop.

Kinetics for  $\gamma$ -GluABA of the dimer loop mutant enzymes T35A, S36A, P39A, S41A, S42A, and E43A did not significantly change compared to wild-type, showing that the dimer loop does not affect the allostery of hGS.

Thermal stability studies show that all the dimer loop mutant enzymes except S36A have a decrease in thermal stability. The slight increase in thermal stability compared to wild-type indicates a slightly more stable hGS enzyme, which could be attributed to increased hydrogen bonds at the dimer interface when mutating the serine to an alanine, but this cannot be fully explained presently.

Dimer loop mutant enzymes have changes in  $\gamma$ -GluABA substrate affinity, indicating that these dimer loop mutants impact the active site of hGS. Dimer loop mutants S36A and S41A have a decrease binding affinity for  $\gamma$ -GluABA, which correlates to the mutant enzymes decrease in activity, S36A (down 17%) and S41 (down 23%). Dimer loop mutant enzymes P39A and S42A have an increase in binding affinity for  $\gamma$ -GluABA, that may cause a decrease in product formation which leads to the decrease in hGS activity of P39A and S42A.

Dimer loop mutants do not affect the allostery of hGS, but do decrease in hGS activity and stability (except S36A). Dimer loop residue P39 plays a particularly key role in the loop, as seen by its large decrease in enzyme activity and thermal stability when mutated to an alanine.

## CHAPTER V

### FUTURE DIRECTION

A continued study of the allostery of hGS is ongoing within the Anderson group. While single point mutations of the dimer loop and dimer interface residues S42, R221 and D24 did not affect the allostery of hGS, other residues have been more promising and have shown to alter the allostery of hGS. Currently, a computational study on identifying the specific allosteric pathway of hGS is being undertaken.

Future research will focus on three loops located at the active site of hGS. These three loops envelope the  $\gamma$ -glutamyl substrate, and therefore may participate in substrate binding and may be responsible hGS allostery.

## REFERENCES

- Adair, G.S. (1925) The hemoglobin system. VI. The oxygen dissociation curve of hemoglobin. *J. Biol. Chem.* 63, 529-545.
- Altschul, S.F., Madden, T.L., Schäffer, A.A., Zhang, J., Zhang, Z., Miller, W., and Lipman, D.J. (1997) Gapped BLAST and PSI-Blast: a new generation of protein database search programs. *Nucleic Acids Res.* 25, 3389-3402.
- Bains, J.S., and Shaw, C.A. (1997) Neurodegenerative disorders in humans: the role of glutathione in oxidative stress-mediated neuronal death. *Brain Res. Rev.* 25, 335-358.
- Becke, A. D. (1993) Density-functional thermochemistry. III. The role of exact exchange. *J. Chem. Phys.* 98, 5648-5652.
- Berendsen, H., Postma, J., van Gunsteren, W., Hermans, J. Interaction models for water in relation to protein hydration (1981) In *Intermolecular Forces*. (Pullman, B., Ed.), pp 331–38. D. Reidel Publishing Company, Dordrecht, Netherlands.
- Berendsen, H.J.C., van der Spoel, D., and van Drunen, R. (1995) GROMACS: a message-passing parallel molecular dynamics implementation. *Comp. Phys. Comm.* 91, 43-56.
- Berman, H.M., Westbrook, J., Feng, Z., Gilliland, G., Bhat, T.N., Weissig, H., Shindyalov, I.N., and Bourne, P.E. (2000) The protein data bank. *Nucleic Acids Res.* 28, 235-42.  
([www.pdb.org](http://www.pdb.org))

- Bohr, C., Hasselbach, K.A., and Krogh A. (1904) *Skand. Arch. Physiol.* *16*, 402 – 412
- quoted in Koshland, D.E., Jr., and Hamadani, K. (2002) Proteomics and models for enzyme cooperativity. *J. Biol. Chem.* *277*, 46841-46844.
- Brown, T. R., Drummond, M. L., Barelier, S., Crutchfield, A. S., Dinescu, A., Slavens, K. D., Cundari, T. R., and Anderson, M. E. (2011) Aspartate 458 of human glutathione synthetase is important for cooperativity and active site structure. *Biochem. Biophys. Res. Comm.* *411*, 536-542.
- Calleja, V., Laguerre, M., and Larijani, B. (2009) 3-D structure and dynamics of protein kinase B-new mechanism for the allosteric regulation of an AGC kinase. *J. Chem. Biol.* *2*, 11–25.
- Cornell, W.D., Cieplak, P., Bayly, C.I., Gould, I.R., Merz, K., Ferguson, D.M., Spellmeyer, D.C., Fox, T., Caldwell, J.W., Kollman, P.A. (1995) A second generation force field for simulation of proteins, nucleic acids, and organic molecules. *J. Am. Chem. Soc.* *117*, 5179-5197.
- Cui, Q., and Karplus, M. (2008) Allostery and cooperativity revisited. *Protein Sci.* *17*, 1295-307.
- Dinescu, A., Anderson, M.E., and Cundari, T.R. (2007) Catalytic loop motion in human glutathione synthetase: a molecular modeling approach. *Biochem. Biophys. Res. Commun.* *353*, 450-456.

- Dinescu, A., Brown, T.R., Barelier, S., Cundari, T.R., and Anderson, M.E. (2010) The role of the glycine triad in human glutathione synthetase. *Biochem. Biophys. Res. Commun.* 400, 511-516.
- Dinescu, A., Cundari, T.R., Bhansali, V.S., Luo, J.L., and Anderson, M.E. (2004) Function of conserved residues of human glutathione synthetase. *J. Biol. Chem.* 279, 22412–22421.
- Fawaz, M.V., Topper, M.E., and Firestone, S.M. (2011) The ATP-grasp enzymes. *Bioorg. Chem.* 39, 185-191.
- Franci, M.M., Pietro, W.J., Hehre, W.J., Binkley, J.S., Gordon, M.S., DeFrees, D.J. and Pople, J.A. (1982) A polarization basis set for second row elements. *J. Chem. Phys.* 77, 3654-3665.
- Galperin, M.Y., and Koonin, E.V. (2012) Divergence and convergence in enzyme evolution. *J. Biol. Chem.* 287, 21-28.
- Galperin, M.Y., and Koonin, E.V. (1997) A diverse superfamily of enzymes with ATP-dependent carboxylate-amine/thiol ligase activity. *Protein Sci.* 6, 2639-2643.
- Geitmann, M., Elinder, M., Seeger, C., Brandt, P., de Esch, I.W.J., and Danielson, U.H. (2011) Identification of a novel scaffold for allosteric inhibition of wild type and drug resistant HIV-1 reverse transcriptase by fragment library screening. *J. Med. Chem.* 54, 699-708.
- Goodey, N., and Benkovic, S.J. (2008) Allosteric regulation and catalysis emerge via a common route. *Nature Chem. Bio.* 4, 474-482.

- Gutheil, W.G. (1992) Thermodynamic model of cooperativity in a dimeric protein: unique and independent parameters formulation. *Biophys. Chem.* 45, 181–191.
- Haber, J.E., and Koshland D.E., Jr. (1967) Relation of protein subunit interactions to the molecular species observed during cooperative binding of ligands. *Proc. Natl. Acad. Sci. USA.* 58, 2087-2093.
- Hasinoff, B. B., and Davey, J. P. (1986) Pig heart fumarase really does exhibit negative kinetic co-operativity at a constant ionic strength. *Biochem. J.* 235, 891-893.
- Hehre, W.J., Ditchfield, R., and Pople, J.A. (1972) Self—consistent molecular orbital methods. XII. Further extensions of Gaussian—type basis sets for use in molecular orbital studies of organic molecules. *J. Chem. Phys.* 56, 2257-2261.
- Hendsch, S.Z. and Tidor, B. (1994) Do salt bridges stabilize proteins? A continuum electrostatic analysis. *Protein Sci.* 3, 211-226.
- Henis, Y. I., and Levitzki, A. (1980) The sequential nature of the negative cooperativity in rabbit muscle Glyceraldehyde-3-phosphate dehydrogenase. *Eur. J. Biochem.* 112, 59-73.
- Hess, B., Kutzner, C., van der Spoel, D., and Lindahl, E. (2008) GROMACS 4: algorithms for highly efficient, load-balanced, and scalable molecular simulation. *J. Chem. Theory Comput.* 4, 435-447.
- Huang, C., He, W., Meister, A., and Anderson, M. E. (1995) Amino acid sequence of rat kidney glutathione synthetase. *Proc. Natl. Acad. Sci.* 92, 1232-1236.

- Jez, J. M., and Cahoon, R.E. (2004) Kinetic Mechanism of Glutathione Synthetase from *Arabidopsis thaliana*. *J. Biol. Chem.* 279, 42726-42731.
- Jones, S., and Thornton, J.,M. (1996) Principles of protein-protein interactions. *Proc. Natl. Acad. Sci. USA.* 93, 13-20.
- Jones, S., and Thornton, J.M. (1995) Protein-protein interactions: a review of protein dimer structures. *Prog. Biophys. Molec. Bio.* 63, 31-65.
- Kalodimos, C.G. (2012) Protein function and allostery: a dynamic relationship. *Ann. N.Y. Acad. Sci.* 1260, 81-86.
- Kantrowitz, E.R. (2012) Allostery and cooperativity in Escherichia coli aspartate transcarbamoylase. *Arch. Biochem. Biophys.* 519, 81-90.
- Keskin, O., Gursoy, A., Ma, B., and Nussinov, R. (2008) Principles of protein-protein interactions: what are the preferred ways for proteins to interact? *Chem. Rev.* 108, 1225-1244.
- Kirtley, M.E., and Koshland, D.E., Jr. (1967) Models for cooperative effects in proteins containing subunits. Effects of two interacting ligands. *J. Biol. Chem.* 242, 4192-4205.
- Koshland, D. E., Jr., and Hamadani, K. (2002) Proteomics and models for enzyme cooperativity. *J. Biol. Chem.* 277, 46841-46844.
- Koshland, D.E., Jr. (1996) The structural basis of negative cooperativity: receptors and enzymes. *Curr. Opin. Struct. Biol.* 6, 757-761.



- Larsson, A., Ristoff, E., and Anderson, M.E., Glutathione synthetase deficiency and other disorders of the  $\gamma$ -glutamyl cycle (2005) *In* Metabolic Basis of Inherited Disease, Online (genetics.accessmedicine.com) (Scriver, C.R., Beaudet, A.L., Sly, W.S., and Valle, D., Eds.) McGraw Hill, New York
- LiCata, V.J., and Allewell, N.M. (1998) Solvent perturbation of the allosteric regulation of aspartate transcarbamylase. *Biochim. Biophys. Acta.* 1384, 306-314.
- Lowry, O.H., Rosebrough, N.J., Farr, A.L., and Randall, R.J. (1951) Protein measurement with the folin phenol reagent. *J. Biol. Chem.* 193, 265–275.
- Luo, J.L., Huang, C.S., Babaoglu, K., and Anderson, M.E. (2000) Novel kinetics of mammalian glutathione synthetase: characterization of gamma-glutamyl substrate cooperative binding. *Biochem. Biophys. Res. Commun.* 275, 577–581.
- Meister, A. (1974). Glutathione synthesis. *In* The Enzymes (P. D. Boyer, Ed.), pp. 671–697. Academic Press, New York
- Meister, A., and Anderson, M. E. (1983) Glutathione. *Annu. Rev. Biochem.* 52, 711–760.
- Meng, E.C., Pettersen, E.F., Couch, G.S., Huang, C.C., and Ferrin, T.E. (2006) Tools for integrated sequence-structure analysis with UCSF Chimera. *BMC Bioinformatics.* 7, 339.
- Min, W., Jiang, L., and Xie, X.S. (2010) Complex kinetics of fluctuating enzymes: phase diagram characterization of a minimal kinetic scheme. *Chem. Asian J.* 5, 1129-1138.
- MOE (Molecular Operating Environment) Chemical Computing Group Inc.,  
<http://www.chemcomp.com>.

- Newton, A.C., and Koshland, D. (1989) High cooperativity, specificity, and multiplicity in the proteinkinase C-lipid interaction. *J. Biol. Chem.* 264, 14909-14915.
- Nieland, T.J.F., Xu, S., Penman, M., and Krieger, M. (2011) Negatively cooperative binding of high-density lipoprotein to the HDL receptor SR-BI. *Biochemistry* 50, 1818-1830.
- Oppenheimer, L., Wellner, V.P., Griffith, O.W., and Meister, A. (1979) Glutathione synthetase purification from rat kidney and mapping of the substrate binding sites. *J. Biol. Chem.* 254, 5184-5189.
- Polekhina, G., Board, P.G., Gali, R.R., Rossjohn, J., and Parker, M.W. (1999) Molecular basis of glutathione synthetase deficiency and a rare gene permutation event. *EMBO J.* 12, 3204-3213.
- Rader, A.J., and Brown, S.M. (2011) Correlating allostery with rigidity. *Mol. Biosyst.* 7, 464-471.
- Ristoff, R., and Larsson, A. (2002) Oxidative stress in inborn errors of metabolism: lessons from glutathione deficiency. *J. Inherit. Metab. Dis.* 25, 223-226.
- Ruzicka, F.J., and Frey, P.A. (2010) Kinetic and spectroscopic evidence of negative cooperativity in the action of lysine 2,3-aminomutase. *J. Phy. Chem. B* 114, 16118-16124.
- Schmidt, M.W., Baldridge, K.K., Boatz, J.A., Elbert, S.T., Gordon, M.S., Jensen, J.J., Koseki, S., Matsunaga, N., Nguyen, K.A., Su, S., Windus, T.L., Dupuis, M., and Montgomery, J.A. (1993) General atomic and molecular electronic structure system. *J. Comput. Chem.* 14, 1347-1363.

- Slavens, K.D., Brown, T.R., Barakat, K.A., Cundari, T.R., and Anderson, M.E. (2011) Valine 44 and valine 45 of human glutathione synthetase are key for subunit stability and negative cooperativity. *Biochem. Biophys. Res. Commun.* 410, 597-601.
- Swain, J.F., and Gierasch, L.M. (2006) The changing landscape of protein allostery. *Curr. Opin. Struct. Bio.* 16, 102-108.
- Tomasi, J., Mennucci, B., and Cammi, R. (2005) Quantum mechanical continuum solvation models. *Chem. Rev.* 105, 2999-3093.
- Townsend, D.M., Tew, K.D., and Tapiero, H. (2003) The importance of glutathione in human disease. *Biomed. Pharmacother.* 57, 145-155.
- Tzeng, S., Kalodimos, C.G. (2011) Protein dynamics and allostery: an NMR view. *Curr. Opin. Struct. Biol.* 21, 62-67.
- Urwyler, S., and Sibley, D.R. (2011) Allosteric modulation of family C G-protein coupled receptors: from molecular insights to therapeutic perspectives. *Pharmacol. Rev.* 63, 59-126.
- van der Spoel, D., Lindahl, E., Hess, B., Groenhof, G., Mark, A.E., and Berendsen, H.J.C. (2005) GROMACS: fast, flexible and free. *J. Comput. Chem.* 26, 1701-1718.
- Wells, J.A., McClendon, C.L. (2007) Reaching for high hanging fruit in drug discovery at protein-protein interfaces. *Nature.* 450, 1001-1009.
- Winkle, S. A., and Krugh, T. R. (1981) Equilibrium binding of carcinogens and antitumor antibiotics to DNA: Site selectivity, cooperativity, allostery. *Nucleic Acids Res.* 9, 3175-3186.

- Xu, D., Tsai, C., and Nussinov, R. (1997) Hydrogen bonds and salt bridges across protein-protein interfaces. *Protein Eng.* 10, 999-1012.
- Yamaguchi, H., Kato, H., Hata, Y., Nishioka, T., Kimura, A., Oda, J., and Katsube, Y. (1993) Three-dimensional structure of the glutathione synthetase from *Escherichia coli* B at 2.0 Å resolution. *J. Mol. Biol.* 229, 1083-1100.
- Yu, E.W., and Koshland, D.E., Jr. (2001) Propagating conformational changes over long (and short) distances in proteins. *Proc. Natl. Acad. Sci. USA.* 98, 9517-9520.
- Zhuravlev, P.I., and Papoian, G.A. (2010) Protein functional landscapes, dynamics, allostery: a tortuous path towards a universal theoretical framework. *Quart. Rev. Biophys.* 43, 295-332.